2003

Simulation of the Variability in Microelectronic Capacitors having Polycrystalline Dielectrics with Columnar Microstructure

jesse Cousins

SIMULATION OF THE VARIABILITY IN MICROELECTRONIC CAPACITORS HAVING POLYCRYSTALLINE DIELECTRICS WITH COLUMNAR MICROSTRUCTURE

By

Jesse L. Cousins

B.S. University of Maine, 2000

A THESIS

Submitted in Partial Fulfillment of the

Requirements for the Degree of

Master of Science

(in Electrical Engineering)

The Graduate School

The University of Maine

December, 2003

Advisory Committee:

David E. Kotecki, Associate Professor of Electrical and Computer Engineering, Advisor

Donald M. Hummels, Professor of Electrical and Computer Engineering

John Vetelino, Professor of Electrical and Computer Engineering

SIMULATION OF THE VARIABILITY IN MICROELECTRONIC CAPACITORS HAVING POLYCRYSTALLINE DIELECTRICS WITH COLUMNAR MICROSTRUCTURE

By Jesse L. Cousins

Thesis Advisor: David E. Kotecki

An Abstract of the Thesis Presented
in Partial Fulfillment of the Requirements for the
Degree of Master of Science
(in Electrical Engineering)
December, 2003

Increasing circuit densities drive the search for microelectronic capacitors with smaller areas. One solution which reduces capacitor size while leaving capacitance constant is to use a thin film of a high permittivity material such as Ta_2O_5, $SrTiO_3$ (STO), or (Ba,Sr)TiO_3 (BST), whose dielectric constants are much higher than those of currently used dielectrics such as SiO_2 and Si_3N_4. One drawback of these dielectric films is that they have a polycrystalline microstructure and the permittivity and leakage current density depend on grain size and orientation. It is unknown how microstructure variations will affect the variability and yield of devices incorporating these films. We have developed a Monte Carlo computer simulation to investigate the variability in capacitance and leakage of microelectronic capacitors incorporating polycrystalline dielectrics. Statistical distributions of crystal area, capacitance, and leakage were evaluated. A capacitance model was developed based on permittivity variation versus crystal grain size, and a leakage model was developed based on the Schottky model of electron injection, taking into account barrier height variation versus crystal grain size and barrier height lowering as a function of permittivity. For one simulation, the capacitor area was varied between 0.001 μm^2 and 0.3 μm^2, and two million capacitors were generated. For

the second series of simulations lognormal crystal grain area probability distributions were used to simulate the same range of capacitor areas. The results were then analyzed for trends in how the capacitance and leakage of polycrystalline capacitors will vary based on the innate variations of the dielectrics, independently of any process variations. It was found that variability decreased as the average crystal size became small relative to total capacitor size. Capacitance variations ranged from 3% to 129% and leakage variations ranged from 0.09% to 386% depending upon the size of the capacitor and the crystal area probability distribution used. For capacitors with amorphous dielectrics, these variations would not exist.

ACKNOWLEDGMENTS

This thesis was supported by the University of Maine Department of Electrical and Computer Engineering with funding from the University of Maine Office of Research and Sponsored Programs.

I would like to thank my mother for her support and guidance while I studied at The University of Maine. I would also like to thank Alfred Doyle for his friendship and support.

Thank you, Dave Kotecki, for your guidance, insight, and patience during this project. Thank you, John Vetelino, for giving me the solid state background to understand what's happening in these dielectrics. Finally, thank you, Don Hummels, for the statistics training that showed me how to set up these simulations and interpret the results.

TABLE OF CONTENTS

LIST OF TABLES

LIST OF FIGURES

CHAPTER 1

INTRODUCTION

1.1 Background

Microelectronic circuit development has been driven by advances in lithography which has reduced the minimum feature size of devices and interconnects. Circuits with smaller feature size consume less space, operate at higher frequencies, require less power, and enable the manufacture of more complex circuits. Semiconductor manufacture costs are relatively constant per wafer, so the cost of making a product is dependent upon the percentage of wafer area the die occupies. In addition, larger circuits have a greater chance of having processing defects which render the circuit inoperable.

Capacitors are vital components in modern integrated circuits. They are used as passive elements in analog designs and as decoupling capacitors to provide a source of charge in digital designs. Dielectric thin films are also used as gate dielectrics for field effect transistors. Reducing the area of capacitors while keeping the capacitance values the same would allow higher device density, thus permitting smaller chips with identical functionality, as well as allowing the practical manufacture of devices which would be too large to be economically feasible with current technologies.

A typical microelectronic capacitor consists of two highly conductive single crystalline or doped polycrystalline electrodes with a layer of Si_3N_4 or SiO_2 dielectric sandwiched between them. The relative permittivity of these commonly used dielectrics is between four and seven. The value of capacitance is determined by the thickness of the dielectric and the surface area of the electrodes. As the thickness of the dielectric is decreased, capacitance increases, but this trend has finite limits. Quantum tunnelling becomes significant for very thin (less than $\sim$1.5 nm) dielectrics, limiting the minimum thickness. In a typical microelectronic process, the thickness of the dielectric is fixed,

leaving a circuit designer to vary the area of the electrodes to achieve the desired capacitance. The area of the electrodes is limited by economic concerns. For these reasons, it is desirable to keep capacitors as small as possible while maintaining the required capacitance. Thus, the maximum capacitance of a process is determined by the minimum thickness of the dielectric and the maximum area a designer is willing to devote to capacitors.

In order to shrink the physical area of a capacitor while keeping the capacitance constant, alternative dielectrics are being explored which have much higher permittivities [1]. One class of dielectrics are paraelectric materials such as Barium Strontium Titanate (Ba_x, Sr_{1-x})TiO_3 (BST) and Strontium Titanate $SrTiO_3$ (STO). Thin films of these materials have very high permittivities in the range of $50-500$. High permittivity is achieved only when these materials have a crystalline or polycrystalline microstructure. Both the permittivity and leakage have been found to be a function of microstructure.

Thin films such as BST and STO can be deposited by sputtering or Chemical Vapor Deposition (CVD) and are commonly produced with a columnar morphology. Currently used dielectrics such as SiO_2 and Si_3N_4 occur as amorphous films. These films have no microstructure; their electrical properties depend only upon the film's thickness. An illustration of an amorphous versus a polycrystalline thin film is shown in Figure 1.1. Figure 1.1(a) is a depiction of an amorphous film and Figure 1.1(b) is a depiction of a polycrystalline film.

One application which utilizes large numbers of capacitors and has low tolerance for capacitance variation is Dynamic Random Access Memory (DRAM). A 1–bit DRAM cell, which contains one transistor and one capacitor, is shown in Figure 1.2. The memory is addressed through the word line, and information is written and read through the bit line. Since the capacitor does not hold its charge indefinitely due to the finite resistance of the dielectric, DRAM cells must be refreshed periodically in order to

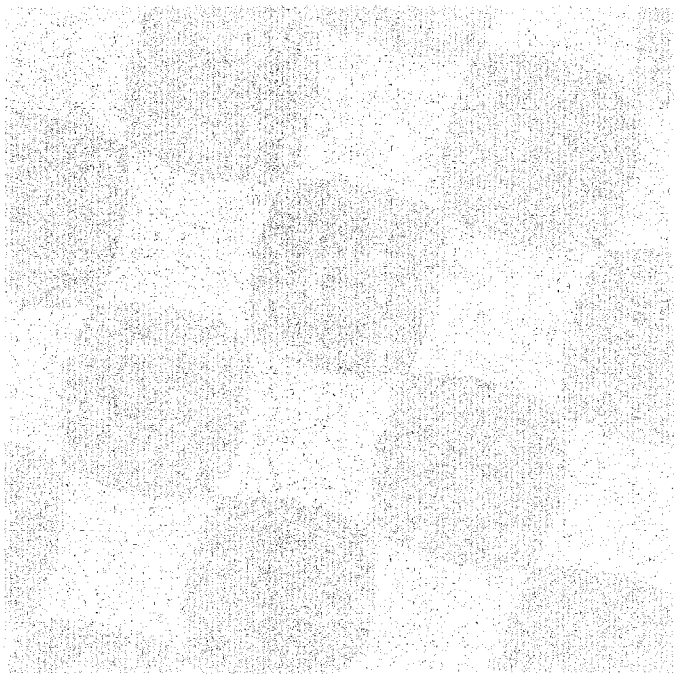

(a) An amorphous film.

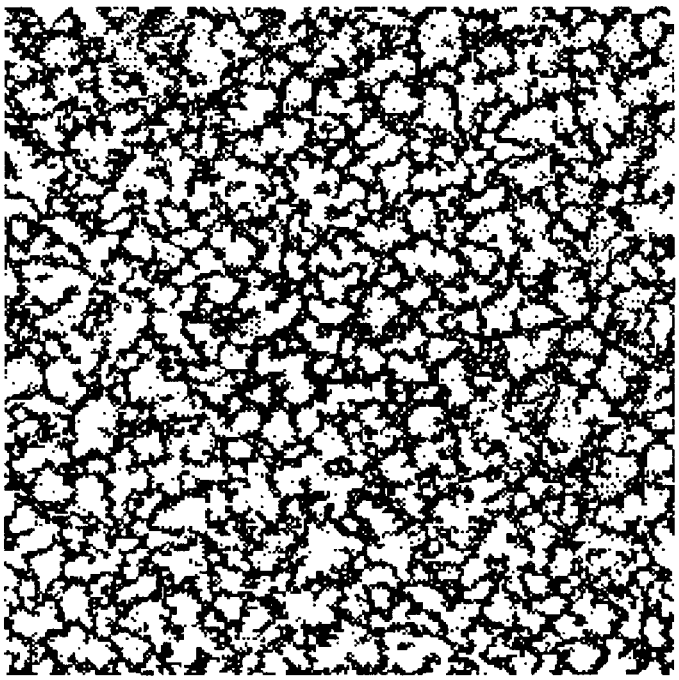

(b) A polycrystalline film.

Figure 1.1: Diagrams showing the difference between a polycrystalline and amorphous film.

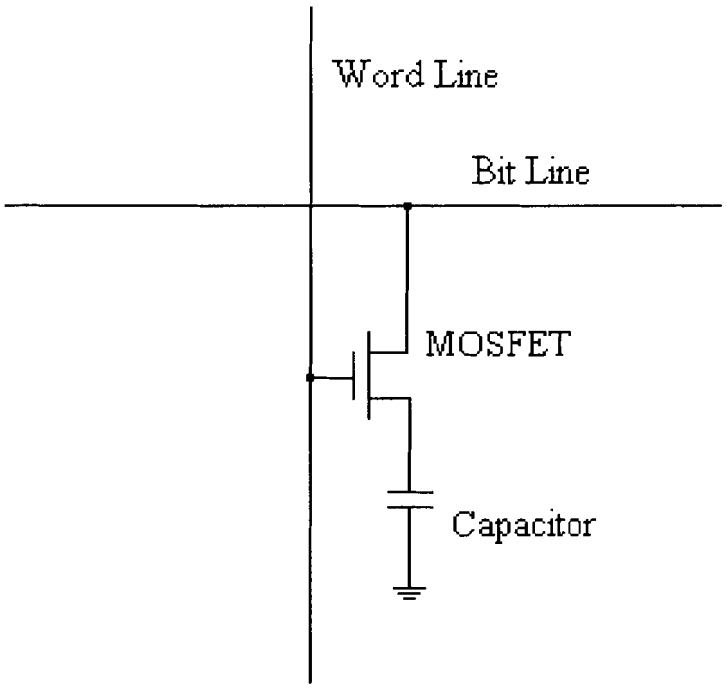

Figure 1.2: Basic DRAM cell: one transistor, one capacitor.

prevent information loss. Refresh rates impose limitations in the values of the capacitance in a DRAM cell. The smallest capacitor on the chip must be large enough that the data is preserved between refresh times; the voltage on the capacitor cannot decay from $\pm$ VDD to the point where the bit value is unknown between refreshes. Reading and clearing information have to be accomplished quickly as well, so maximum capacitance limits are determined by the discharge times. These requirements impose minimum and maximum values of allowable capacitance. All capacitors on a chip must meet these requirements for the chip to be functional.

1.2 Purpose of the Research

Problem: The influence of the microstructure of polycrystalline dielectrics on the capacitance and leakage variation in microelectronic capacitors are unknown.

A capacitor which offers high capacitance for a small physical area is needed. This research is an investigation into whether polycrystalline dielectrics can offer the above without introducing unacceptable variations in capacitance and leakage. A Monte Carlo simulation program was written using C/C++ and Matlab to generate millions of simulated capacitors of a specified area with polycrystalline dielectrics having a microstructure determined by a probability function. The resulting variations in capacitance and leakage was analyzed.

Though immediately significant to the DRAM industry, polycrystalline dielectrics have other uses. Polycrystalline dielectrics have potential as decoupling capacitors in ASICs, and could be used as gate oxides in MOSFETs. DRAM and gate oxide applications have the narrowest reproducibility requirements so simulation results are analyzed with these applications in mind, but should be of interest to anyone interested in using polycrystalline dielectric films in capacitors, regardless of application.

1.3 Review of Prior Work

There have been many works characterizing the electrical behavior of polycrystalline dielectric thin films, and several studies that investigate their potential in DRAM capacitors and as transistor gate dielectrics [1, 2, 3]. There have also been several papers which investigate the properties of DRAM variability, but these models confined themselves to studying transistor variations and assumed the capacitor did not vary [4, 5, 6, 7]. This section outlines relevant prior work.

Three works had significant influence on the simulations presented in this work. Kotecki et al. [2] discussed the preparation of BST films by liquid–source metal–organic chemical vapor deposition (MOCVD) and the physical and electrical characteristics of deposited films. They found that specific capacitance and charge loss are strongly dependent upon a variety of process parameters. These simulations make use of TEM

images from this paper to give a probability density function for crystal size. Ezhilvalavan and Tseng [1] present an overview of progress in BST for DRAM applications. They cover deposition techniques, physical, electrical, and dielectric properties, effects of different electrode materials, and reliability, among others. Their bibliography is comprehensive and many examples of BST films are presented in their paper. The data on permittivity versus average crystal size used in the simulations is based upon data from this work. Dietz et al. [3] performed a comprehensive review of leakage currents in a $(Ba_{0.7}, Sr_{0.3})TiO_3$ film grown by MOCVD. They concluded that the Schottky model accounts for the material's resistive properties at high electric fields but barrier lowering behavior is not accurately described at high fields. The Schottky approximation and leakage values from Dietz et al. are used to model leakage behavior in this work – they are discussed in more detail in Chapter 2.

Other works which investigate the same themes include Hamamoto et al. [4], who investigated retention time distributions for conventional DRAM cells. They found that the number of failing cells is dependent upon the boron concentration of the memory cell region, and proposed a thermionic field emission current concept to explain the distribution of failing cells. Hiraiwa et al. [5] used statistical modeling to examine the retention time of conventional DRAM, assuming that retention time is determined by a junction leakage current at carrier traps. Results of Monte Carlo simulations agreed well with experimental results. Restle et al. [6] investigated variations in retention time over time. They measured retention times of several samples from different manufacturers and technologies, then repeated the measurement to investigate whether retention time was varying over time. They found that it was, and described several models to explain this variation. Ogasawara et al. [8] investigate leakage variation in conventional DRAM. They propose a physical model where leakage variation is primarily due to a variation of local electric field strength enhancement. Romanenko and Gosney [7] performed a numerical simulation of leakage in DRAM capacitors having SiO_2 and

Si_3N_4 dielectrics. Direct tunnelling and Fowler–Nordheim leakage mechanisms are used to model leakage through the SiO_2 film, while at high temperatures the Poole–Frenkel effect and state hopping of thermally excited electrons at low temperatures are used to model leakage through Si_3N_4. They vary temperature and dielectric thickness, and display thicknesses for optimal storage time at several temperatures. Shigyo et al. [9] present simulations of MOSFETs and BSIM3v3 parameters generated by inputting random process conditions and known process tolerances. They applied their results to estimations of worst–case performance of DC inverter characteristics and data–out of DRAM. Note that none of these articles address the primary focus of this work, the role of polycrystalline dielectrics in capacitor variation.

This work has been partially presented in other publications. The research presented involved understanding capacitor variation [10] and probability density function variation [11] effects. This document supersedes and encompasses prior work by the author on this subject.

1.4 Thesis Organization

This thesis is organized as follows.

- Chapter 1 introduces the reader to the problem and the research described herein.
- Chapter 2 outlines the assumptions used in the simulations, describes some properties of capacitors having polycrystalline dielectrics with columnar microstructure, and shows the specific capacitance and leakage models used in the simulations.
- Chapter 3 describes the Monte Carlo simulation code which generates capacitors and how data is input and output.
- Chapter 4 exhibits and analyzes the results of the Monte Carlo code.

- Chapter 5 summarizes the data, presents conclusions, and offers suggestions for future work on this project.

CHAPTER 2

THEORY

2.1 Introduction

This section describes the theory used to develop models of microelectronic capacitors having polycrystalline dielectrics with columnar microstructure. We would like to simulate a capacitor with a polycrystalline dielectric and compute its electrical characteristics. To do this the capacitor is divided into many small sections, each consisting of two ideal electrodes and a single crystal grain of the dielectric. Because it is assumed that the dielectric has a columnar microstructure, each crystal extends completely from one electrode to the other, with no crystal boundaries parallel to the electrodes. This assumption is backed up by experimental data [2]. The areas of all the electrodes in the single-grained capacitors will (if the area between crystal grains is neglected) add up to the total area of the capacitor. Since capacitors in parallel add, the sum of the capacitance of each grain-sized device will be the capacitance of the whole, and the leakage current through each grain will add to give the total leakage current of the capacitor.

The capacitors are simulated using a Monte Carlo method, which involves assembling systems or items by randomly selecting from a pool of available building blocks. This application required a range of crystal grain areas and a statistical description of how likely any area would be generated, known as a probability density function (pdf). It was also necessary to develop models for capacitance and leakage current density as a function of the crystal area. Using these equations the Monte Carlo program tracks the electrical and physical properties of the simulated capacitor. These models were based on previously published experimental results [1, 2, 3]. The simulations used a lognormal distribution function to approximate the probability density function of an

arbitrary dielectric. Barium strontium titanate (Ba_x, Sr_{1-x})TiO_3 (BST) thin film data was used as a basis for these simulations due to the large amount of published research available concerning BST. BST occurs in a tetragonal unit cell, with Ba^{2+} or Sr^{2+} at the edges of the cube, O^{2-} at the faces of the cube, and Ti^{4+} at the center of the cube.

Several assumptions were used to reduce the complexity of the simulations. The crystals were assumed to be columnar in shape, and each crystal was assumed to reach completely from one electrode to the other. Detailed geometry of each crystal was neglected. A note on nomenclature: this paper will refer to crystal area, which is meant to be the area in a plane parallel to the plates of a capacitor, and thickness or depth, which is meant to be the distance between the plates. In cases where data was presented using a radius rather than area, it was assumed that the crystal was a solid cylinder oriented with electrodes contacting the circular planes at either end of the cylinder.

The models developed may not be self-consistent. Leakage, permittivity, and probability functions were found using published results which studied different films. This is acceptable since the purpose of this paper is to investigate general trends, not to evaluate a specific process, so while numerical values may be inaccurate, trends should be accurately portrayed.

2.2 Electrical Properties of Capacitors With Polycrystalline Dielectrics

2.2.1 Capacitance

One of the most significant properties of high permittivity thin films is that their dielectric constant ϵ_r has been found to vary with crystal area. A capacitor made up exclusively of larger crystals would thus have much higher capacitance than one consisting of smaller crystals. For example, Figure 5 in [1] shows the average dielectric constant versus grain size radius for several different BST films. The relationship

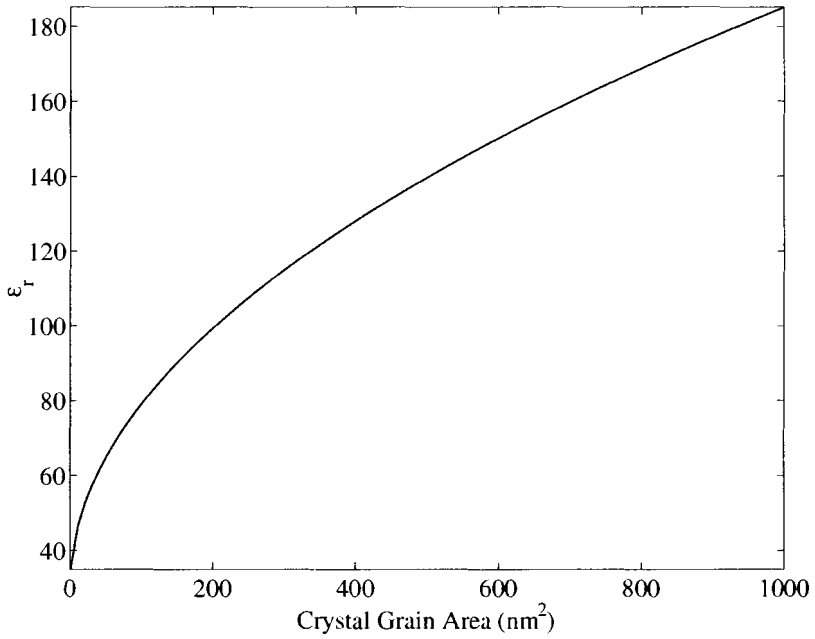

Figure 2.1: The relation between crystal area and ϵ_r used in the simulations.

between ϵ_r and crystal radius is approximated with a first-order polynomial function which when written in terms of the crystal area results in Equation 2.1

$$\epsilon_r = \frac{200}{46}\left[\sqrt{\frac{4A}{\pi}}\right] + 30, \tag{2.1}$$

where ϵ_r is the relative permittivity and A is the crystal surface area in nm^2. Figure 2.1 plots the dielectric constant versus crystal area used in all the simulations.

The equation for a parallel plate capacitor's capacitance C is given by Equation 2.2, where A is the cross-sectional area, ϵ_0 is the permittivity of free space, ϵ_r is the relative permittivity of the material, and d is dielectric thickness.

$$C = \frac{A\epsilon_0\epsilon_r}{d} \tag{2.2}$$

Equation 2.3 relates crystal grain area to crystal capacitance, and is easily found by substituting Equation 2.1 into Equation 2.2. Equation 2.3 is shown in Figure 2.2.

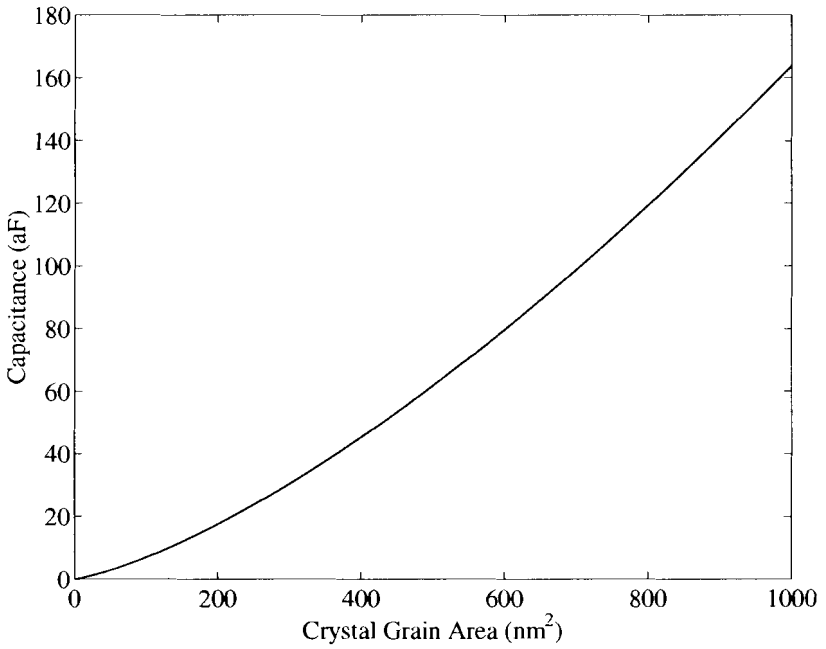

Figure 2.2: The relation between crystal area and capacitance used in the simulations.

$$C(A) = \frac{A\epsilon_0}{d}\left[\frac{200}{46}\left(\sqrt{\frac{4A}{\pi}}\right) + 30\right] \tag{2.3}$$

2.2.2 Leakage

Leakage current density is critical in determining the suitability of capacitors for any application. Leakage current density in this application is current that flows between the plates of a capacitor. It is often approximated by a resistor in parallel with the capacitor. It determines retention time as well as the AC impedance of the capacitor. Characterizations of BST thin films have shown that a Schottky leakage model, given by Equation 2.4, approximates the leakage behavior [3].

$$J = A^{**}T^2 \exp\left(\frac{\alpha_i(A_i)\,E^{\frac{1}{2}}}{kT} - \frac{W_b}{kT}\right) \tag{2.4}$$

where

$$\alpha_i = \left(\frac{q^3}{4\pi\epsilon_0\epsilon_r(A_i)} \right)^{\frac{1}{2}} \tag{2.5}$$

In Equation 2.4, J is the leakage current density in amps per unit area, A^{**} is the effective Richardson constant, T is the temperature, E is the applied electric field, k is the Boltzmann constant, W_b is the zero-field barrier height, ϵ_0 is the permittivity of free space, ϵ_r is the relative permittivity of the dielectric, and A_i is the crystal's cross–sectional area. In Equation 2.5, q is the charge on an electron. It should be noted that extraction of the Richardson constant and barrier height lowering from experimental data do not produce realistic values for a BST thin film; this is discussed briefly in other sources [3]. Nevertheless, the experimental data is well approximated by the functional form of the Schottky model.

Leakage measurements have varied even more than capacitance in reported characterizations of BST and other high permittivity thin films. For comparison purposes two different leakage models were used in the simulations. Both models were developed by fitting Equation 2.4 to published data [3].

The modified Schottky model is described by Equation 2.6.

$$J = L_1 \left[\exp\left(\frac{\alpha_i(Ai)\, E^{\frac{1}{2}}}{kT} \right) \right] \tag{2.6}$$

This first model, referred to as leakage model A, represented a best case scenario where leakage was nearly constant with respect to grain size. The experimentally measured leakage current density of $6.3 * 10^{-8}$ A/cm^2 at a field of 270 kV/cm and temperature of 398 K is used to determine the constant $L_1 = 3.33 * 10^{-8}$ A/cm^2[3].

The second leakage model, referred to as leakage model B, incorporated more known values into the exponential portion, and is described in Equation 2.7.

$$J = L_2 \left[\exp\left(\frac{L_3\, \alpha_i(A_i)\, E^{\frac{1}{2}}}{kT} \right) \right] \tag{2.7}$$

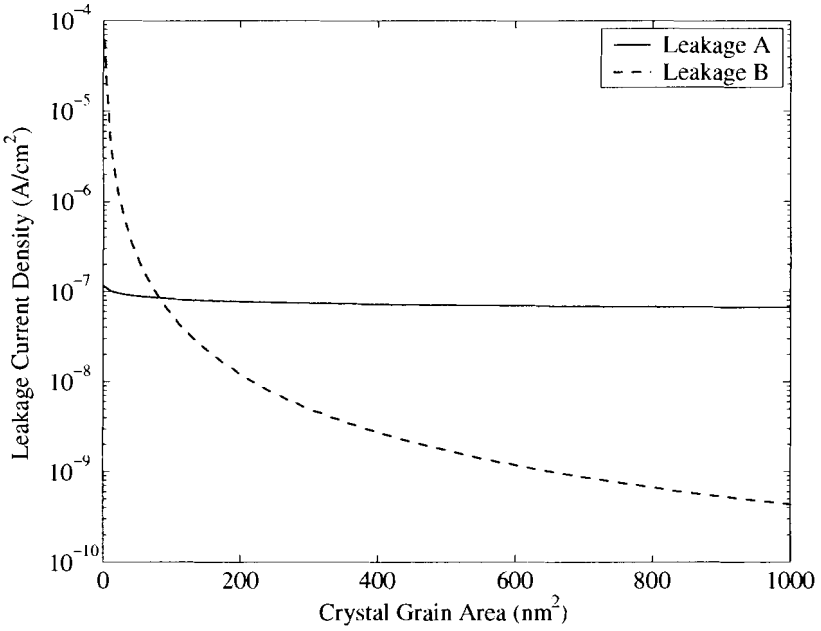

Figure 2.3: Two functions for leakage vs. crystal grain area.

The constants L_2 and L_3 are determined from the intercept and slope of a graph of $E^{\frac{1}{2}}$ vs. ln(J) [3]. The values obtained for L_2 and L_3 are $8.3 * 10^{-13}$ A/cm^2 and 22.1 respectively. This model represents a worst case variation; actual values are likely to be somewhere between the two models. Graphs of the two functions are plotted in Figure 2.3.

2.3 Crystal Size Variation

In addition to modelling how the electrical properties of a film vary with area, it was necessary to model how crystal area distribution would vary from capacitor to capacitor. This was done in two different manners. First, crystal areas were measured manually from a transmission electron microscope (TEM) image of a BST film [2] and a probability density function was fit to the measured data. For a second series of simulations, a lognormal distribution was used in order to provide an easily manipulated probability density function as described in Section 2.3.2.

2.3.1 Experimental Distribution

The experimental distribution was found by manually measuring the areas of crystals in a primarily (100) oriented BST film[2]. BST forms in either (100) or (110) orientations, and it appears that capacitance is not affected by orientation. Leakage may be affected, but it is not understood how[3]. The data points were sorted in ascending order and a non-normalized cumulative distribution function was generated by computing the cumulative sum and plotting it as a function of individual grain area. The value of the function at the largest crystal size was normalized to 1 to generate a cumulative distribution function for the film's crystal area. The value of the cumulative distribution function at a crystal area represents the likelihood that a random crystal will be less than or equal to that area. A polynomial was fit to the cumulative distribution function, and the derivative of that function was taken to generate a probability density function. The average crystal area of this distribution is 108nm^2 and the standard deviation is 76nm^2. The minimum and maximum crystal area are 5.1 and 332 nm^2, respectively. The polynomial fit is given by Equation 2.8:

$$y(A) = -(4.0*10^{-9})A^4 + (6.1*10^{-6})A^3 - (2.9*10^{-3})A^2 + 0.41A + 10\,(nm^2) \quad (2.8)$$

where $y(A)$ is the cumulative density and A is the crystal area in nm^2. The cumulative distribution function and polynomial fit are plotted in Figure 2.4. The derivative of the cumulative distribution function is the probability density function, which is shown in Figure 2.5.

2.3.2 Approximated Lognormal Distribution

In addition to the experimentally determined distribution described in Section 2.3.1, a distribution was needed whose standard deviation σ^2 could be varied to study σ's

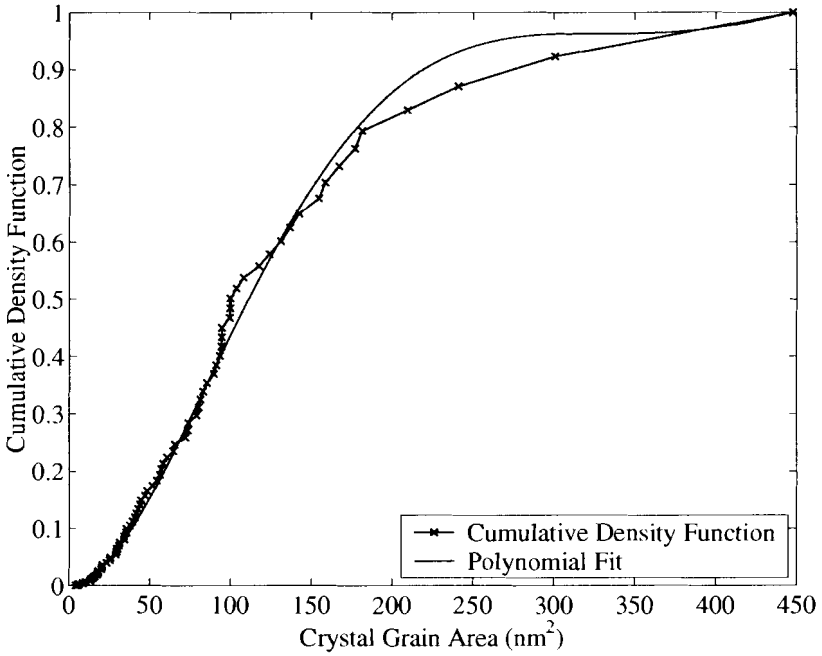

Figure 2.4: Cumulative distribution function and polynomial fit for a BST film.

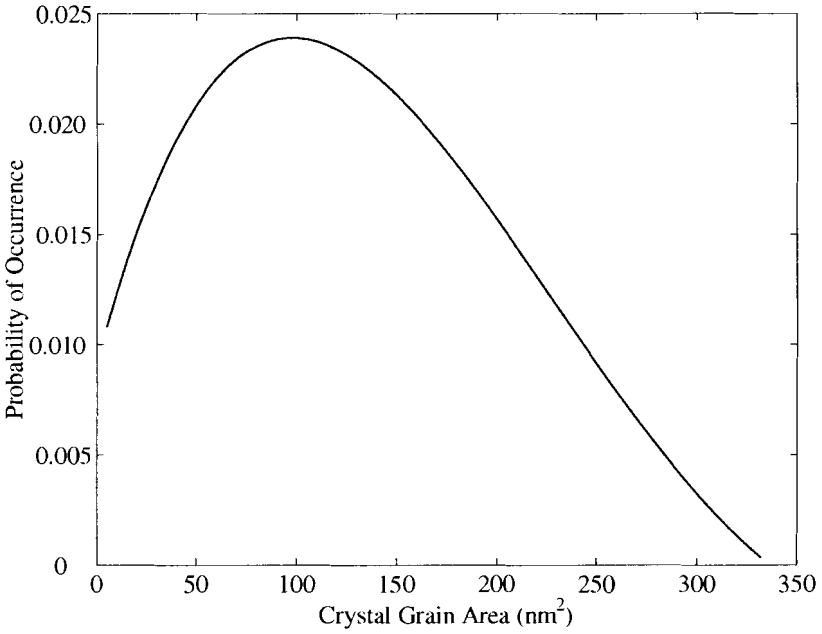

Figure 2.5: Probability density function found using the polynomial fit from Figure 2.4 as the cumulative distribution function.

effects on capacitance and leakage. A lognormal distribution was chosen for its ease of manipulation, the fact that it only exists for positive number values, and close match to the experimental data. The lognormal distribution's probability density function $f_X(x)$ is a function of crystal area in nm^2 given by Equation 2.9:

$$f_X(x) = \frac{1}{S\,x\,\sqrt{2\pi}} \exp\left(\frac{-\left(\ln x - M\right)^2}{2\,S^2}\right) \tag{2.9}$$

where M and S are constants which are linked to the values of the lognormal mean $\bar{X}$ and variance σ^2 of the function as indicated by Equations 2.10 and 2.11:

$$\bar{X} = \exp\left(M + \frac{S^2}{2}\right) \tag{2.10}$$

$$\sigma^2 = \exp\left(2\,M + S^2\right)\left(\exp\left(S^2\right) - 1\right) = \bar{X}^2\left(\exp\left(S^2\right) - 1\right) \tag{2.11}$$

These equations simplify into an expression for the standard deviation σ given by Equation 2.12.

$$\sigma = \bar{X}\sqrt{\exp\left(S^2\right) - 1} \tag{2.12}$$

Lognormal probability distributions were generated for σ = 5, 10, 25, 50, 100, 200, and 300 and used to study the effect of increasing the standard deviation of crystal area while leaving the mean crystal area the same. The distributions are shown in Figure 2.6 with mean area of 100 nm^2, which was chosen since it was close to the experimental distribution's mean area of 108 nm^2. Note that for functions with large values of σ, a greater percentage of the curve is lost on either side of the limits, arbitrarily set at 0.1 and 1000 nm^2 respectively.

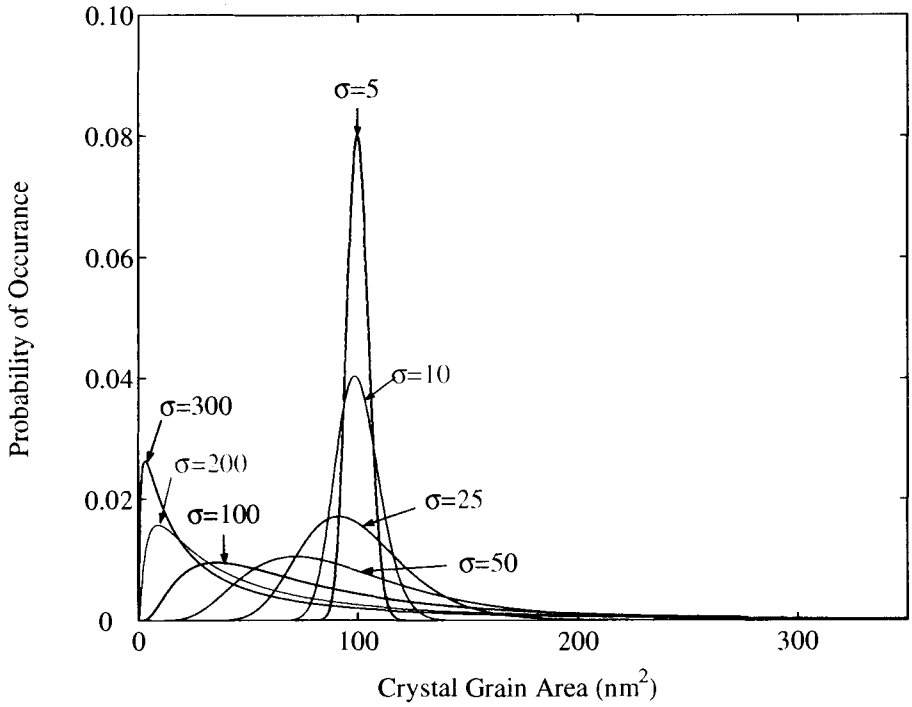

Figure 2.6: Lognormal probability density functions used in the simulations.

CHAPTER 3

SIMULATION METHODOLOGY

3.1 Introduction

This section outlines how the data described in Chapter 2 was used to generate capacitors having a microstructure consistent with a grain size distribution. It covers how probability and electrical data were prepared, how the output data was formatted for analysis, and describes the operation of the capacitor simulation software.

3.2 General Considerations

Chapter 2 provides relationships between the crystal area and the electrical properties, as well as how the distributions of crystal area vary. Software design decisions were made based on the complexity of the formulas as well as the following items:

1. The Monte Carlo simulations would be time- and processor-intensive.
2. Capacitance and leakage calculations would be highly repetitive and inefficient if they were embedded in the Monte Carlo simulation program.
3. The equations described in Chapter 2 could be easily manipulated in Matlab.

The repetitiveness of the calculations was a major factor in the decision to precalculate as much as possible. Calculating the electrical properties of individual crystals during selection would have increased simulation time enormously. It had been decided to use C for the Monte Carlo simulator, and random integers with flat probability distributions (a distribution where all values between two endpoints were equally likely) were easily generated in that language. However, converting a flat distribution to one of the distributions shown in Figures 2.5 and 2.6 would have been as complicated and time consuming as computing capacitance and leakage. Because of this complexity, it was

decided to enter calculated crystal areas with associated electrical properties into the Monte Carlo code and have the simulation code randomly select from these values rather than generate values on the fly.

3.2.1 Input Data

Disk space was not of concern for crystal area data, but for performance reasons it was desired to have all data on a film in memory at the same time. The simulations which used the extracted probability density function of Figure 2.5 had an array of 442,121 values and took approximately fifteen minutes to simulate; the simulations which used the lognormal probability density functions had arrays of between 223,000 and 273,000 values and took approximately 10 minutes.

These data files were saved to disk as newline delimited ASCII text. When a Monte Carlo simulation was performed, data was first read in on the film being simulated. Every line was read into a different element of an array, and the line/array position served as the indexing value. The program would randomly find a value between one and the end of the array and incorporate the area, capacitance, and leakage at the random value into a capacitor.

3.2.2 Output Data

The program outputs data into multiple files containing capacitance, leakage, and number of crystals per capacitor. Two million capacitors were generated per simulation. Using a similar indexing scheme to the input data, each simulated capacitor had an entry for its capacitance and leakage. When varying standard deviation as described in Section 2.3.2, the program created a subdirectory for each probability density function named for its σ. These data files were then read into Matlab for analysis.

3.3 Monte Carlo Simulation

The Monte Carlo simulation code was responsible for taking the data on individual crystals and using it to generate capacitors. A flowchart of the code is shown in Figure 3.1. The code reads film data into memory arrays. If there are multiple probability density functions used, it only loads one film at a time. Two million capacitors of each area defined in the program are randomly generated; if multiple probability density functions are used, the code generates all capacitor areas specified before loading another.

While generating a capacitor, it randomly selects a crystal, then adds the grain's capacitance and leakage to the capacitor's total. When the total area of grains selected is greater than the area desired, the program linearly scales down the area to be exactly the right size. It also linearly reduces the capacitance and leakage by the same factor. For example, if the area was reduced by 1%, the capacitance and leakage would also be reduced by 1%.

Before running, the user must create a working directory with subdirectories for each film, and hard-code what capacitor areas are desired - these simulations used capacitors ranging from 1000 nm^2 to 0.3 μm^2. Films with differing probability density functions need separate directories. The generated data was cached in memory and periodically saved in files. Once all sizes of capacitors for a particular probability density function were generated, memory was cleared and the process repeated with a different distribution.

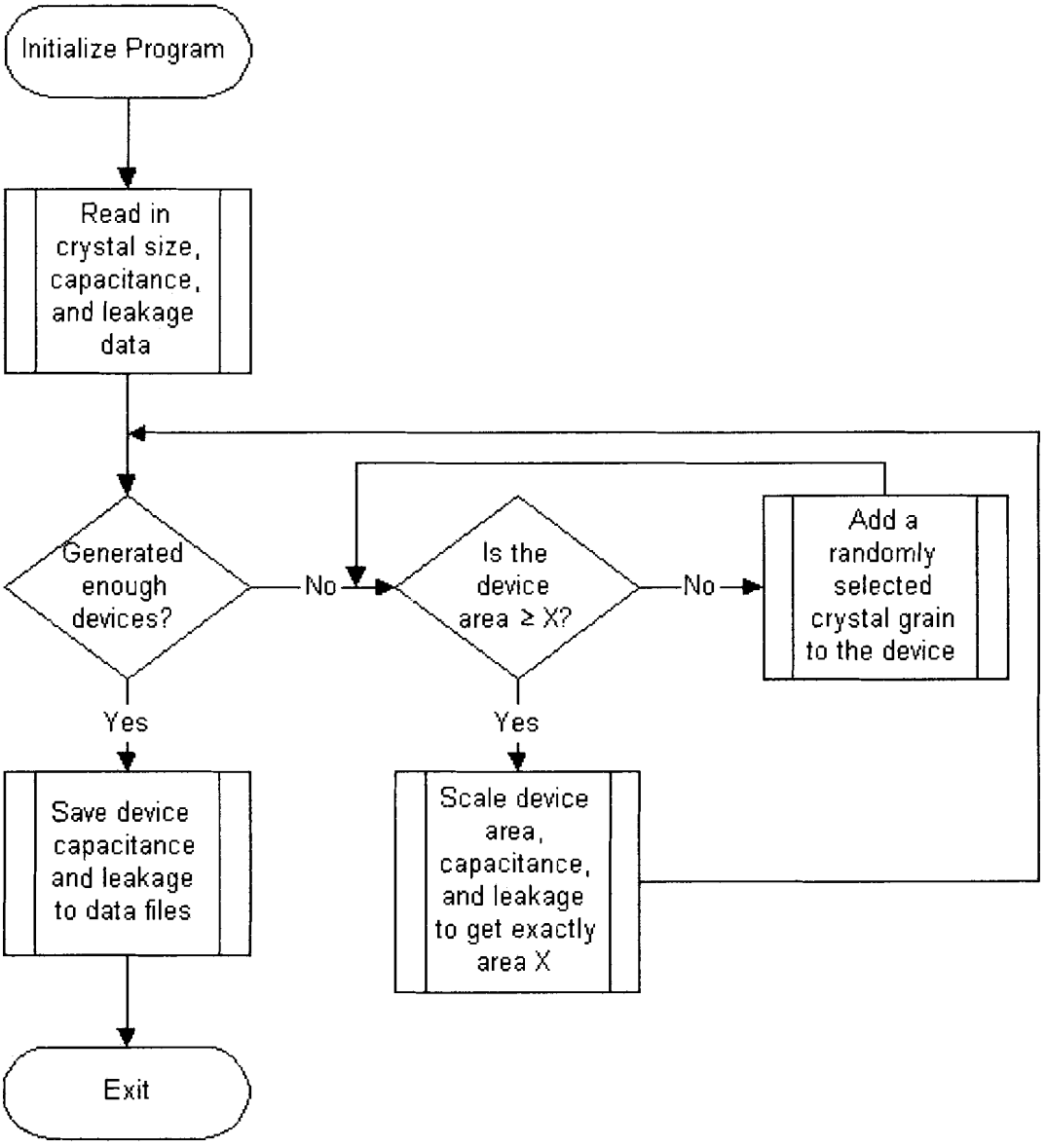

Figure 3.1: Flow chart of the Monte Carlo simulation code.

CHAPTER 4

RESULTS

The results are presented in two different sections. The first discusses the results of varying the capacitor area while using the probability density function shown in Figure 2.5. The second section presents simulations in which lognormal distributions with various standard deviations shown in Figure 2.6 were used to simulate ranges of capacitor sizes with various values of σ. An examination of trends from the simulations should yield insights into capacitor–to–capacitor variations in capacitance and leakage current density for capacitors fabricated with high permittivity polycrystalline dielectrics. Electrical properties in this section are presented in terms of their value per unit area so trends can be more easily compared between different capacitor areas.

4.1 Area Variance With Experimental Distribution

The first series of simulations varied the area of the simulated capacitors from 10 nm^2 to 0.3 μm^2 while keeping the probability density function of crystal sizes constant, using the distribution shown in Figure 2.5. This distribution was based on real-world measurements. The purpose of these simulations was not to determine specific values of capacitance or leakage, but to investigate trends in how these parameters change as the capacitor's area and dielectric film change. Decreasing the mean and standard deviation of crystal area or increasing total capacitor area has the same effect on the trends for the number of crystals per capacitor, so increasing capacitor size will have the same effect on capacitance and leakage trends of capacitors as decreasing mean crystal area.

4.1.1 Capacitance Effects

The minimum, average, and maximum capacitance generated for all capacitor areas can be seen in Figure 4.1. The distance between capacitor electrodes was chosen

to provide an average capacitance density of 30 fF/μm^2. The average number of crystals per capacitor is shown at the top of the graph. For a $0.1\mu m^2$ capacitor, which has approximately 1000 crystals, the minimum and maximum capacitance vary by $\pm 3\%$. This variation is due only to the fundamental variability of the dielectric, without considering normal process variations. Reducing the capacitor area by an order of magnitude increases the variability to $\pm 10\%$ even though there are on average 100 crystals per capacitor. At an area of $10^{-3}\mu$m^2 there are fewer than 10 crystals per capacitor and the predicted variation increases to $\pm 47\%$. Decreasing the thickness or increasing the relative permittivity would increase capacitance density, allowing capacitors with smaller areas to achieve the same capacitance, but the percent variation would not change. Percent variation was calculated as shown by Equation 4.1, where x is the variable in question.

$$Percent\ Variation(x) = \left(\frac{max(x) - min(x)}{average(x)}\right) * 100\% \tag{4.1}$$

4.1.2 Leakage Effects

The simulated percent variation of leakage current density for the two leakage models is shown in Figure 4.2. For DRAM applications, retention targets require a maximum total charge leakage (from the capacitor and the transfer device) of $\sim$ 1fA/μm^2. As can be seen, the two models produced very different results. Leakage model B is a worst case leakage, and produced variations ranging from 59% to 644% as the capacitor area decreases from 0.1 to 0.001 μm^2. Leakage model A was more constant with respect to crystal area, and produced variations from 0.1% to $\sim$30% as the capacitor area decreased from 0.1 to 0.001 μm^2. Even when the average number of crystals per capacitor was greater than 1000, the variation in leakage current density was 43% for leakage model B and was reduced to 0.87% for leakage model A. Decreasing the average number of crystals per capacitor from 1000 to 100 increased the percent variation from

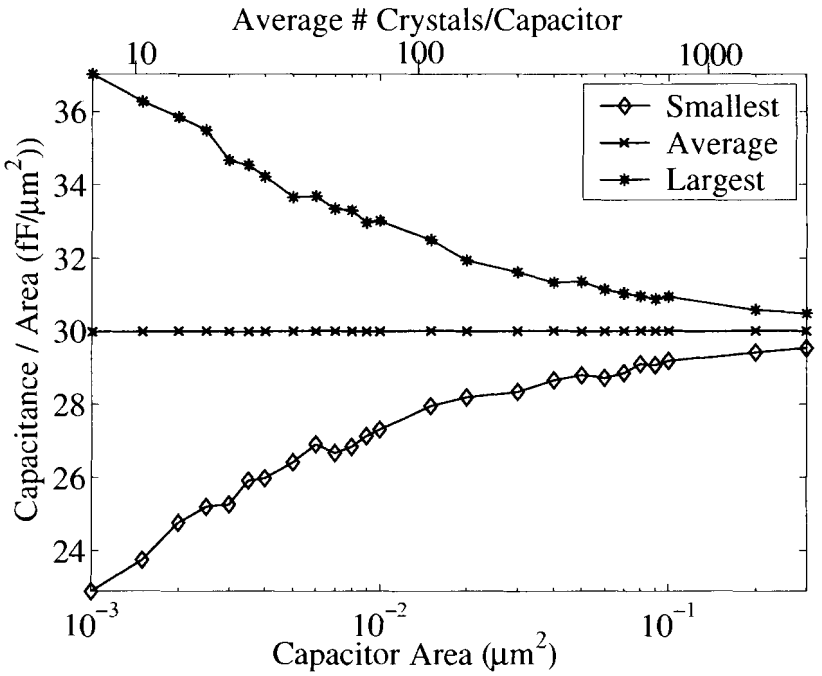

Figure 4.1: Variations in capacitance for capacitors of different areas

43% to 154% for leakage model B and from 0.87% to 4.1% for leakage model A. Decreasing the average number of crystals per capacitor from 100 to 10 increased the percent variation from 154% to 644% for leakage model B and from 4.1% to 27.5% for leakage model A.

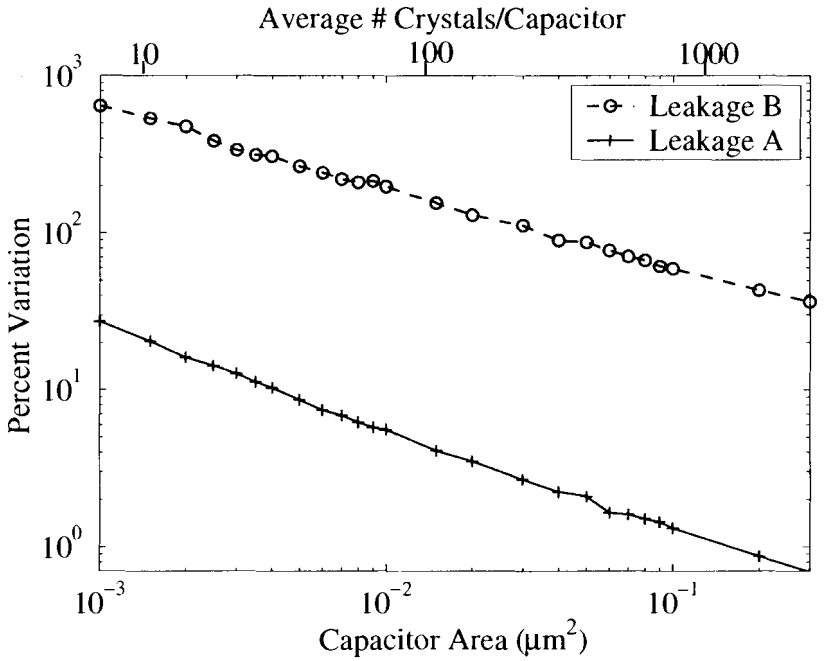

Figure 4.2: Variations in leakage for capacitors of different areas

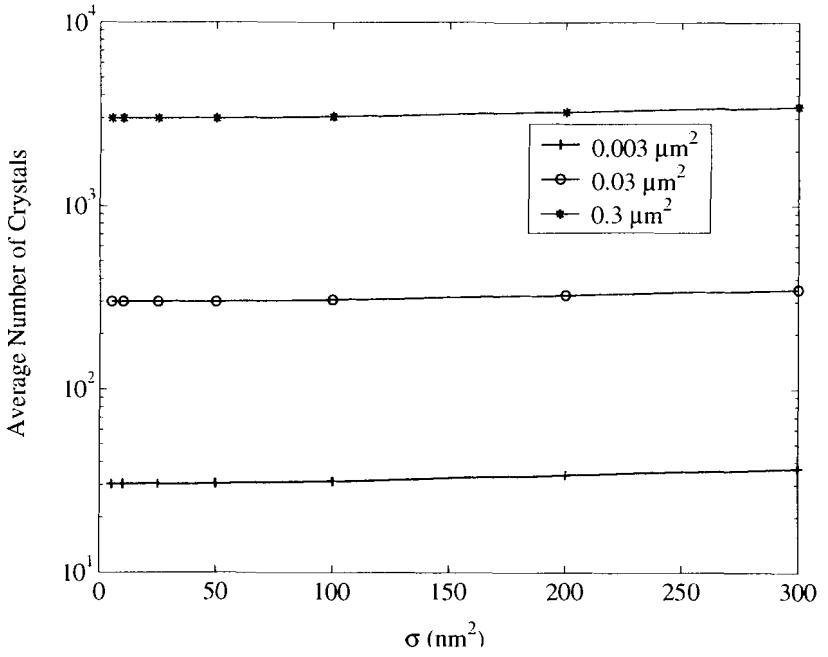

Figure 4.3: The average number of crystal grains per capacitor shifts slightly upward as σ increases.

4.2 Lognormal σ Variation

The final series of simulations used the lognormal probability density functions from Section 2.3.2 to model the crystal area distribution. Each distribution was used to generate the same range of capacitor sizes used in the simulations of Section 4.1. Before electrical properties are discussed, an imperfection in the method of preparing the lognormal distributions should be mentioned. In addition to the electrical properties, the Monte Carlo simulation code saved the number of crystals that made up each capacitor. Figure 4.3 shows how the averages of three capacitor sizes varied with respect to the standard deviation. For a perfect lognormal distribution the average number of crystals should be independent of σ. It can be seen that all three increase slightly as σ increases. This is due to the fact that the lognormal distribution in the simulations has a hard cutoff at the minimum value instead of one that varies as σ increases. This small variation should not effect the overall trends from the results.

Since this series of simulations varied both capacitor area and probability density function, many graphs are necessary to completely represent the data. For brevity, and since capacitor area variation has already been explored in Section 4.1, variations in capacitor area will be highlighted for capacitors with areas of 0.003, 0.03, and 0.3 nm^2.

4.2.1 Capacitance Effects

Figure 4.4 shows the capacitance variation as a function of σ for the 0.3 μm^2 area capacitor. For these simulations, the mean crystal area is maintained at 100 nm. The thickness of the dielectric of the simulated capacitors of every area was scaled so that the mean capacitance produced by the distribution with a standard deviation σ = 100 nm^2 was 30 $fF/\mu m^2$. The results show that minimum capacitance is nearly constant as the standard deviation is increased. Under these conditions, half the crystals generated have areas between 0 and the mean area of 100 nm^2. Over that range permittivity is approximately linear. When sigma becomes large, the permittivity becomes more nonlinear. Thus capacitance per unit area is more constant below than above the mean. This could also be explained by the fact that there are minimum crystal sizes specified in the simulation and that small variations near the maximum number of crystals per capacitor produce negligible capacitance variations in individual capacitors. As the standard deviation goes up, the probability of larger crystals occurring increases, and large crystals contribute much more capacitance than an equivalent area of smaller ones. They also take up more space and reduce the total number of crystals in the capacitor, thus increasing the variability of the capacitor. A constant minimum combined with a rapidly increasing maximum explains why the average capacitance gradually increases as well. This result may also be influenced by trimming the lower bound of the lognormal distribution used in the simulations at a hard value rather than at a multiple of the standard deviation.

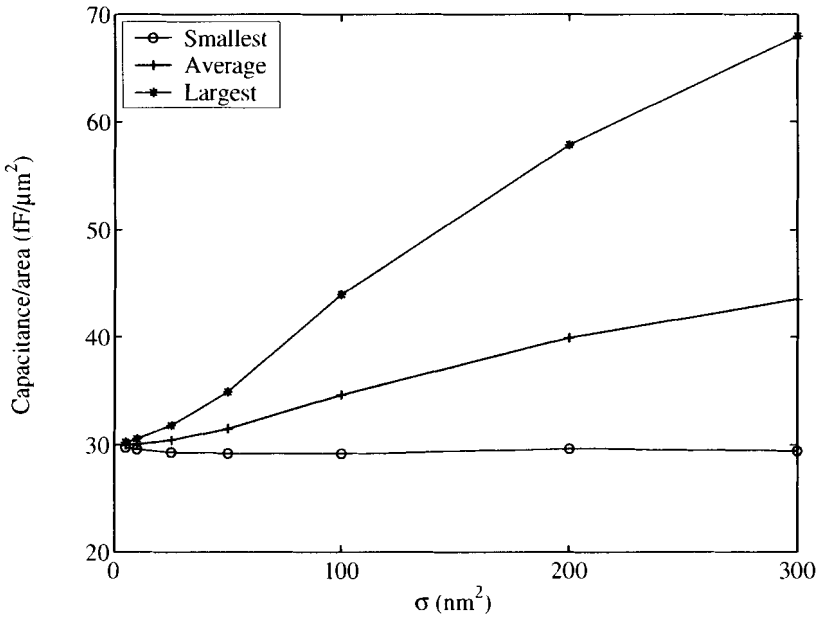

Figure 4.4: This graph illustrates how the minimum, average, and maximum capacitance density of 2,000,000 simulated capacitors changes with respect to σ for the 0.3 μm^2 area capacitor

Figure 4.5 shows the histograms of the capacitance per unit area for the 0.003 μm^2 capacitors simulated with lognormal distributions having standard deviations from 5 to 300. The values of σ refer to the probability distribution function of crystal grain areas and have units of nm. The histograms are formed by taking the total range of capacitance for each σ and dividing it into 500 equally spaced subranges. The number of capacitances that occur in each range is counted and the results plotted on the Y–axis of each graph to produce a histogram which displays information similar to that of a probability density function. Note that this method doesn't produce normalized histograms – the area under each curve is not one. Normalizing the histograms would have made displaying all the histograms on the same Y–axis difficult. The lack of normalization means that percent variation cannot be compared using these histograms, so percent variation will be considered separately. The peak of these histograms represents the mode, or most common observation. Symmetrical functions should have modes close to

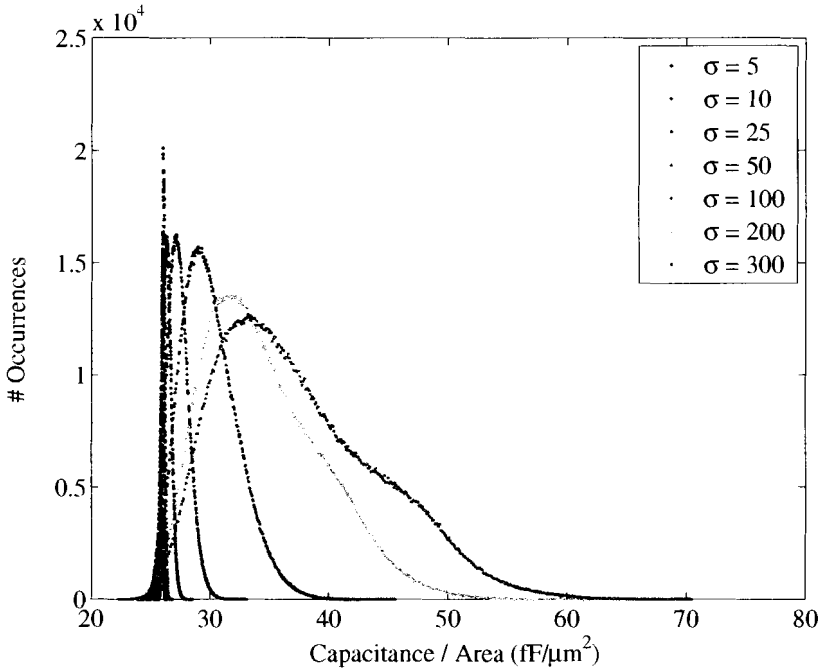

Figure 4.5: Histogram showing how capacitance/area shifts with σ for 2,000,000 capacitors with an area of 0.003 μm^2

the average. The minimum capacitance per unit area diminished slightly as σ increased, ranging from 23 to 26 fF/μm^2 as σ increased from 5 to 300 nm^2. The first two standard deviation plots appear almost as impulse functions compared to the rest. It is no surprise that films which have small standard deviations produce capacitors with small standard deviations. The film with σ = 25 nm^2 is the first one to have any distinguishable shape; the film appears to produce a simple second order polynomial shape. For higher values of σ the histograms are skewed to the left. This supports the idea that the upper outliers have a greater effect on total capacitance.

The distributions in Figure 4.5 look almost lognormal. The shape is due to a property of normal and lognormal distributions, that any system which has as inputs linear operations on lognormal distributions will produce outputs in a lognormal distribution. Though capacitance is nonlinear, it is close enough that it produces nearly lognormal outputs here. As capacitors get larger (increasing the number of inputs) and

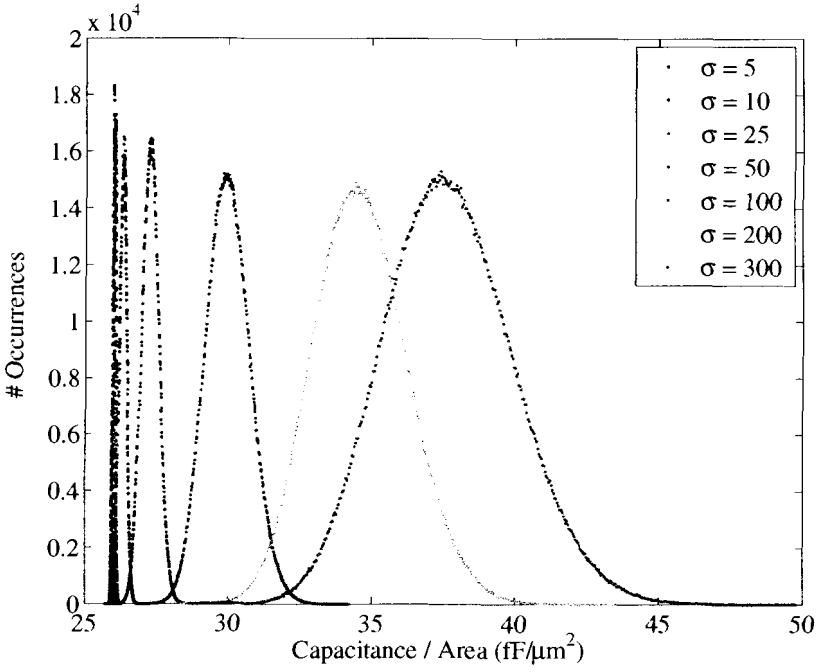

Figure 4.6: Histogram showing how capacitance/area shifts with σ for 2,000,000 capacitors with an area of 0.03 μm^2.

the capacitance gets more nonlinear, this trait will be attenuated and the output should become Gaussian.

Figure 4.6 shows the results of capacitance simulations for a capacitor area of 0.03 μm^2. The σ = 5 and 10 nm^2 distributions have again produced results with very small standard deviations, but the distributions for larger standard deviation show greater distribution–to–distribution variation in capacitance range. For each value of σ, maximum values of capacitance per unit area have decreased, and minimum values have increased. The mode of these distributions appears to be getting larger as the standard deviation increases. Since the mean of all crystal area probability density functions is 100 nm^2, larger crystals must be having a greater effect on final capacitance than smaller ones. The lognormal tendencies can only be seen now by looking at the tails of the distribution and comparing their distance from the median.

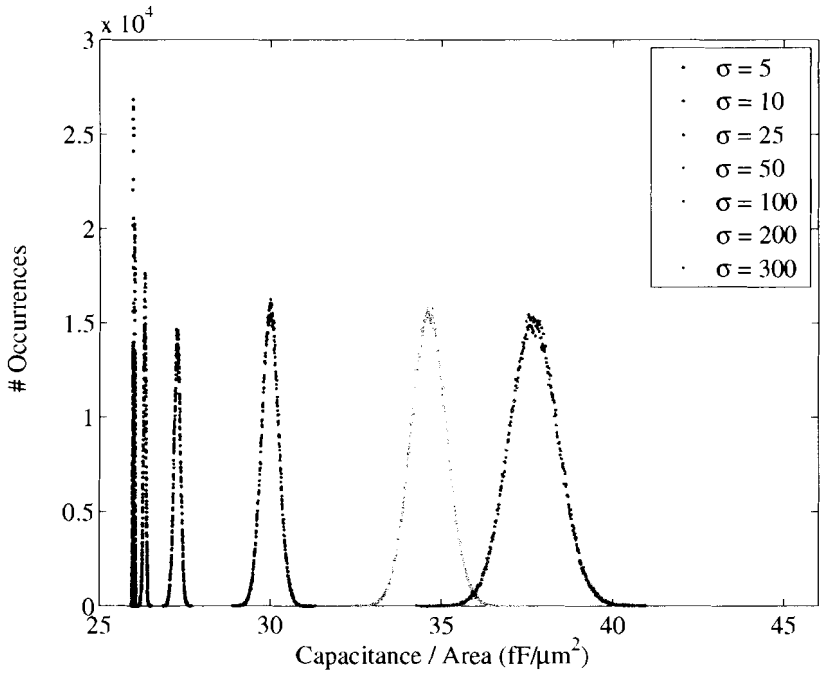

Figure 4.7: Histogram showing how capacitance/area shifts with σ for 2,000,000 capacitors with an area of 0.3 μm^2.

Figure 4.7 show a histogram of the results for a capacitor size of 0.3 μm^2. All visible traces of a lognormal distribution are gone, and the modes of the different values of σ are even more separated. The ranges of min and max capacitance are more narrow, indicating that the standard deviation of capacitance for the capacitors is shrinking. The mean values are close to those in Figure 4.6. Unlike earlier graphs, larger values of σ produce very few results that occur less than 10 times in a subrange, reinforcing the idea that the standard deviation of capacitor capacitance gets smaller as the average crystal area becomes small with respect to total crystal area. The minimum capacitance per unit area for any value of σ is unchanged from the previous graphs at 26 fF/μm^2. This implies that the minimum capacitance per unit area depends only upon mean crystal area, with the standard deviation having no impact.

Figure 4.8 shows how the percent variation in capacitance changes with respect to standard deviation of crystal area. It can be seen that the variation decrease found

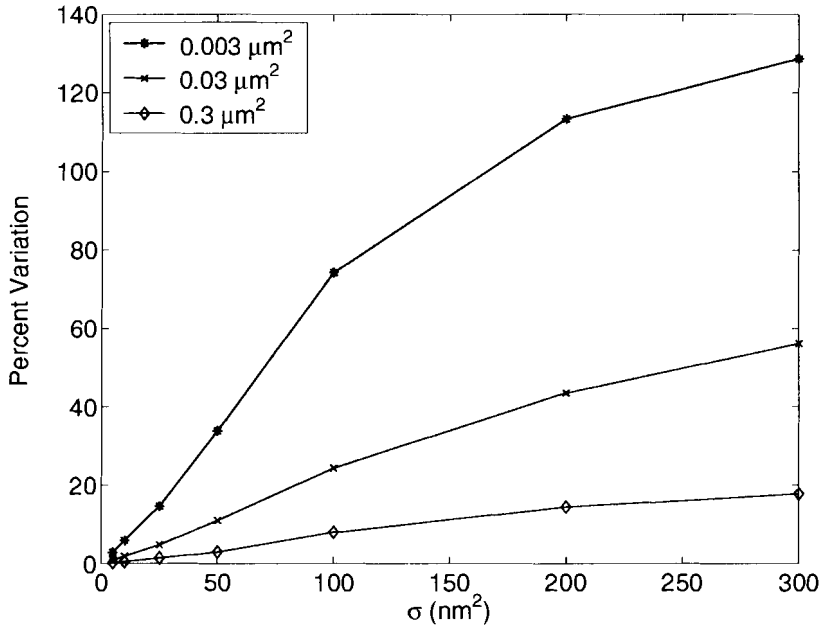

Figure 4.8: Percent variation of capacitance versus σ for three different values of capacitance.

when increasing the area from 0.003 to 0.03 μm^2 is much greater than when increasing from 0.03 to 0.3 μm^2. This shows that in order to control capacitor variation the average number of crystals per capacitor must be kept large. The derivatives of these curves can give some insight into the scaling problem. Notice that for the 0.03 and 0.3 μm^2 capacitors the slopes are constantly decreasing, yet for the 0.003 μm^2 capacitor the slope increases between σ = 25 nm^2 and σ = 100 nm^2, then decreases to match that of the 0.03 μm^2 capacitor between σ = 200 and 300 nm^2. This is the same behavior seen in Figure 4.5.

4.2.2 Leakage Effects

An examination of Figure 4.9 will be helpful in understanding the results in this section. Figure 4.9 shows leakage versus crystal area, unlike Figure 2.3 which shows leakage density versus crystal area. The leakage current density profiles are similar, but the leakage values behave differently. Leakage model A, whose leakage density

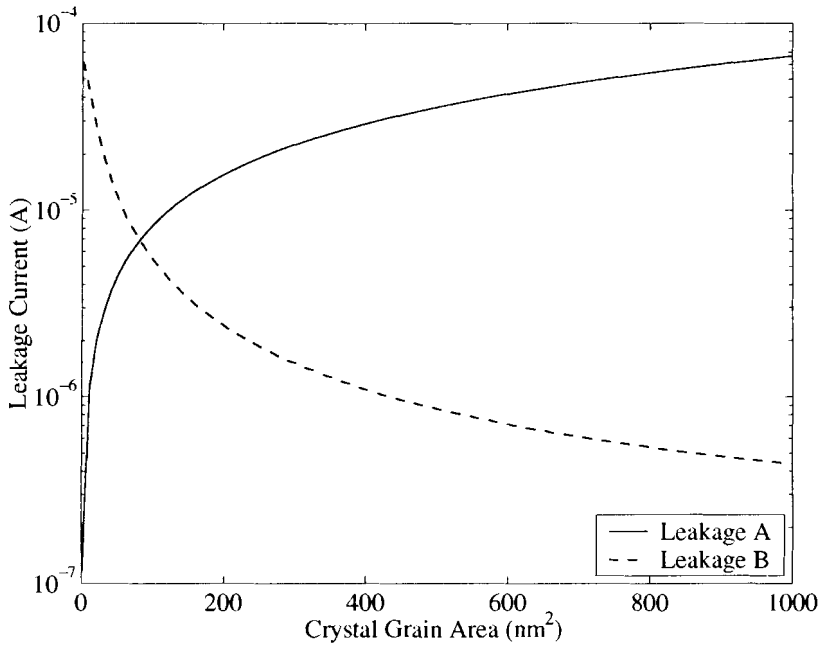

Figure 4.9: Leakage versus individual crystal area.

varied less, has a leakage current which increases rapidly from zero but starts to level off. Leakage model B, whose leakage density varied more, has a leakage current which decreases rapidly from zero but whose rate of decrease levels off. Both the curves start to level off around the mean crystal area of 100 nm^2. For both films, it's apparent that the small crystals will dominate the behavior of capacitors with these films, since they both vary more over areas smaller than the mean than they do larger than the mean. This implies that the average value of leakage current will increase with larger values of sigma for leakage model B and decrease with larger values of sigma for leakage model A.

The histograms in the following sections were prepared by taking the range of each distribution, splitting it evenly into 200 sections, and finding the number of occurrences per section. The variation in ranges over all simulated capacitors made choosing a single section size which didn't distort the data impossible. The areas under each histogram will be different, because each distribution has 2 million data points over a

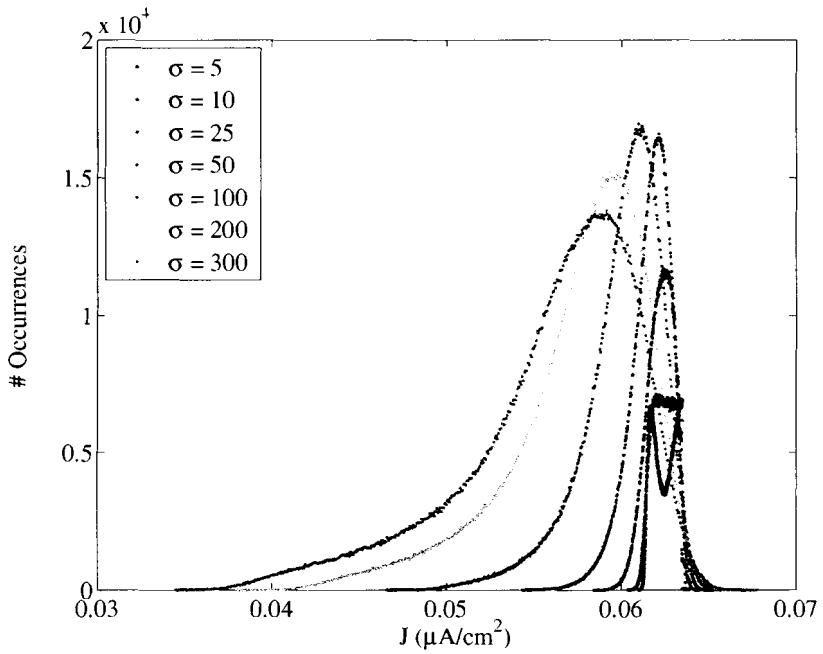

Figure 4.10: Histogram showing how leakage current density shifts with σ for a 0.003 μm^2 capacitor using the minimally varying model A.

range of leakage values unique to it. Normalizing the histograms made displaying them on a linear scale problematic.

4.2.3 Leakage Model A

Variations in leakage using the more constant distribution A are shown in Figure 4.10 for 0.003 μm^2 capacitors. This capacitor area would have on average 30 crystals. Outliers should be most pronounced in this distribution due to the relatively small crystal/capacitor area ratio. Median leakage decreases slightly with standard deviation as expected, and variation increases with standard deviation. Note that maximum leakage is relatively constant for different standard deviations. The results clearly appear to be reversed lognormal distributions. This makes sense since it was predicted in Section 4.2.2 that the average current will decrease with σ due to the dominance of small, low leakage crystals.

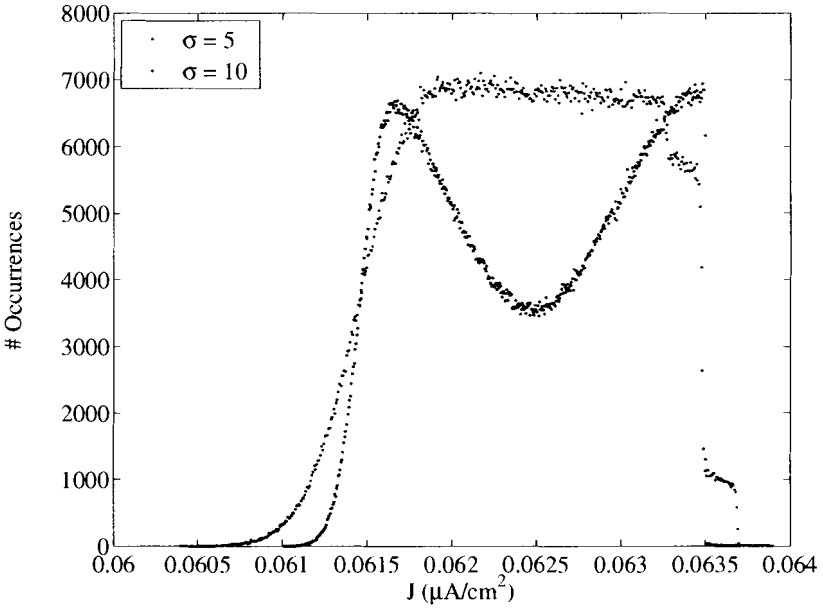

Figure 4.11: Histograms showing $\sigma = 5$ and $\sigma = 10$ from Figure 4.10

Although masked by the other distributions, it can be seen that the distributions produced by films with standard deviations of 5 and 10 nm^2 behave differently than the others. These two distributions are shown separately in Figure 4.11. It is believed that this behavior is the symptom of a limitation in the Monte Carlo simulation software mentioned in Section 3.3. If the final crystal added to a capacitor makes the sum of crystal area in the capacitor larger than desired, all traits are linearly reduced so the total crystal area is exactly as desired. For these two distributions, that scaling has cut into the peak of the lognormal distribution and shifted it down into the tail.

Figure 4.12 shows leakage results for 0.03 μm^2 capacitors. The lognormal distribution appears closer to a normal distribution but skews are still evident upon close inspection. The peaks have become narrower and the modes are closer to each other. Ten times the area of the 0.003 μm^2 capacitor means ten times the number of crystals on average per capacitor, causing greater averaging and less variability in leakage. The capacitors with the film whose standard deviation is 5 nm^2 still behaves differently than those with larger standard deviations. This histogram appears to have two lines, one

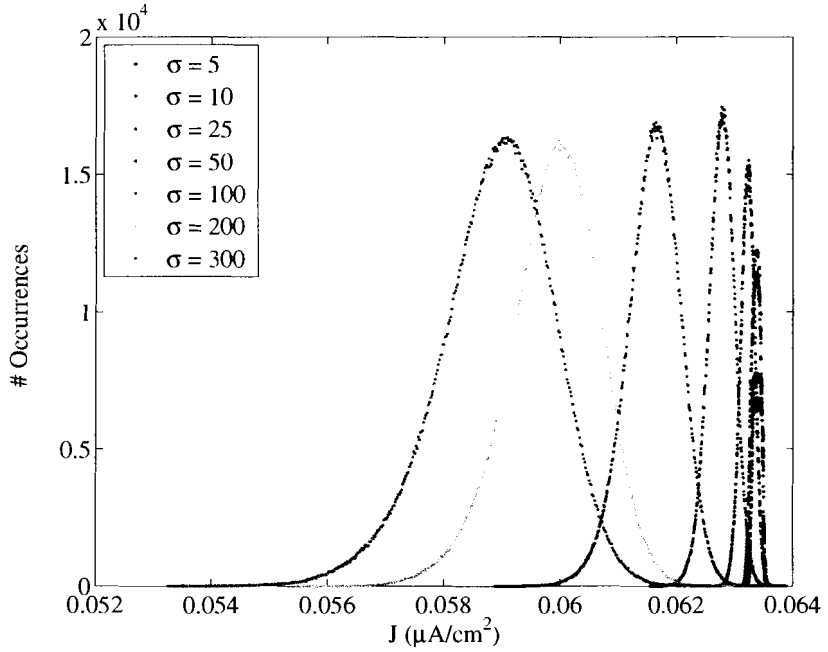

Figure 4.12: Histogram showing how leakage current density shifts with σ for a 0.03 μm^2 capacitor using the minimally varying model A.

over the other, and a large flat peak. Both may still be due to scaling. The broad peak could be the result of the highest leakage capacitors being scaled down. The double line is actually caused by adjacent bins in the histogram having different numbers of occurrences - if the dots were connected the line would proceed in a sawtooth fashion. If this was caused by something which also affected leakage, the lower probability distribution would show some different trait from the higher distribution, such as a skewness or a different mean. Since it does not, this is believed to be caused by the small range of leakage values interfering with the histogram generation. The range is so small that splitting it into 200 sections oversamples the data.

Figure 4.13 shows leakage results for 0.3 μm^2 capacitors. The skewness is even less evident than in Figure 4.12. The distributions are tighter but the mode values are roughly the same as for 4.12. The trend of larger standard deviations producing smaller mode leakage values continues as predicted in Section 4.2.2. Note that while minimum

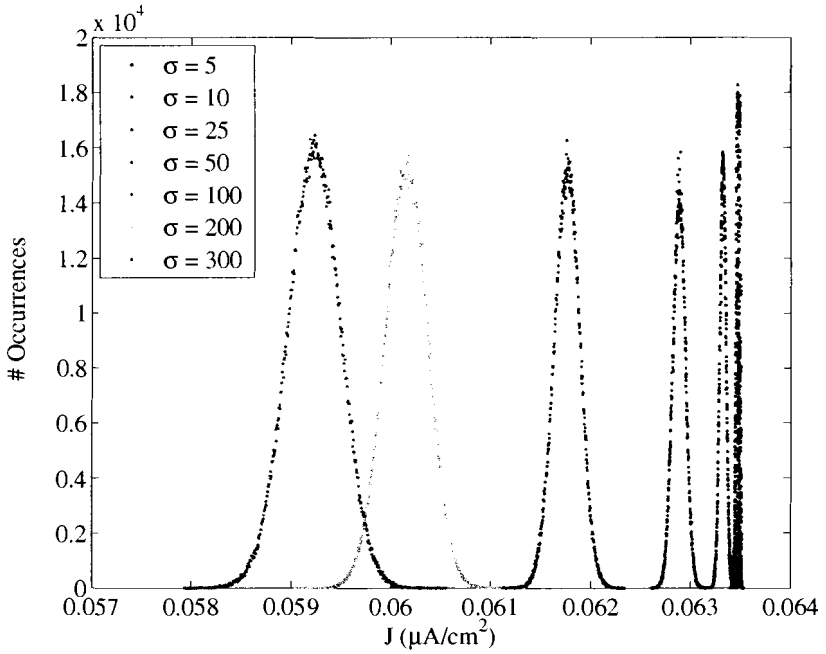

Figure 4.13: Histogram showing how leakage current density shifts with σ for a 0.3 μm^2 capacitor using the minimally varying model A.

leakage has changed quite a bit over the range of capacitor areas, the maximum leakage has been fairly constant.

As usual there is some anomalous behavior for small standard deviations. Figure 4.14 shows only standard deviations of 5 and 10 from Figure 4.13. A sawtooth dual distribution is evident, which suggests oversampling of the data. It is predictable that the largest capacitors made with films that have the smallest variation would have distributions that vary the least.

Figure 4.15 shows the percent variation for the three capacitor sizes versus σ. Contrasting Figure 4.15 with Figure 4.8 shows that worst case variation in leakage is less than half that of capacitance. The variation increased more between the 0.03 and 0.003 μm^2 capacitors – approximately tripling for leakage while nearly doubling for capacitance. All the functions show a lognormal distribution with a mean of approximately 100 nm^2.

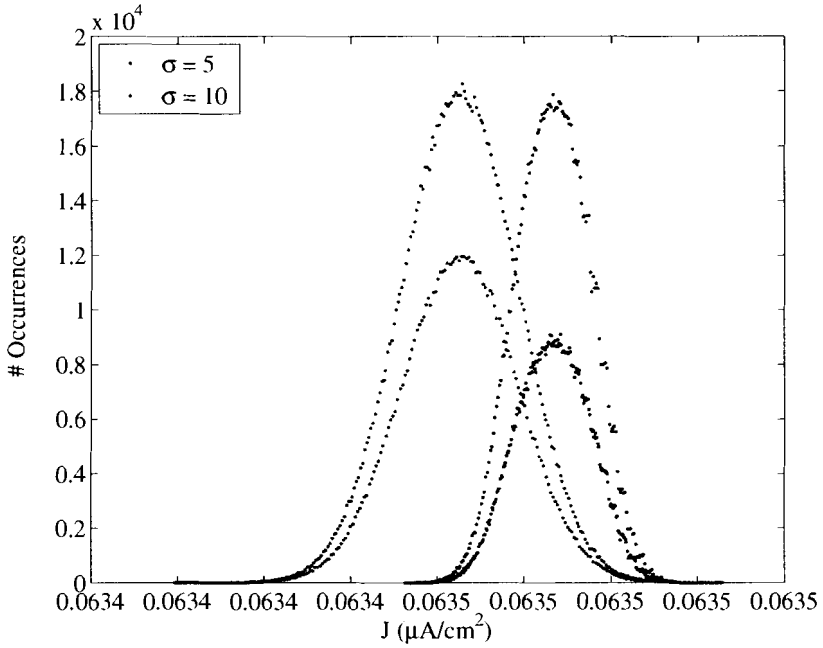

Figure 4.14: Histograms showing σ of 5 and 10 nm^2 from Figure 4.13

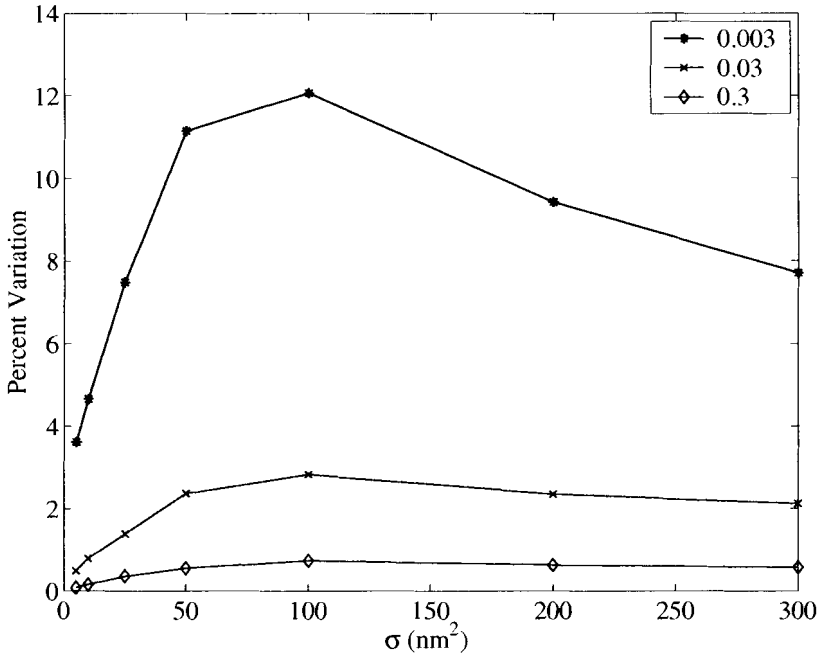

Figure 4.15: Percentage variation of leakage values for three different capacitor areas using the nearly constant leakage model A.

4.2.4 Leakage Model B

Figure 4.16 illustrates the leakage current density of a 0.003 μm^2 capacitor simulated using leakage model B. The prediction in Section 4.2.2 was that average leakage would increase with standard deviation, which it does. Lognormal tendencies can be seen, but are much less evident than in the same capacitors using leakage model A. The minimum leakages found are about the same as in leakage model A for this size, but the maximum values are much greater. This variation, the smoothness of the graphs, and the absence of a dual distribution in the least varying films suggests there's more variation in capacitors simulated with this dielectric model than there was in leakage model A. The values of leakage found are also much more than in capacitors simulated using leakage model A. Leakage model A's 0.003 μm^2 capacitor had a range of $0.035 \mu A/cm^2$, while the same area with leakage model B produced a range of $1.75 \mu A/cm^2$. The mode values for the histograms have also increased. Figure 4.9 shows that the models have nearly the same leakage at the mean size of 100 nm^2, with leakage model A having slightly greater leakage. This shows how the shape of the distribution around the mean can influence devices.

Figure 4.17 shows a zoomed in display of the capacitors generated using the three least varying films. There is no dual distribution, but the histograms are distorted. Their overall Gaussian shape is easier to see than in Figure 4.11. Possibly the distortion is the result of scaling or of leakage model B being more nonlinear than leakage model A.

Figure 4.18 shows the leakage current density of a 0.03 μm^2 capacitor simulated using leakage model B. The range has more than halved from Figure 4.16, but is still more than its leakage model A counterpart in Figure 4.12. As was seen in the other 0.03 μm^2 capacitor, the distributions have tightened, although the mode values haven't changed much.

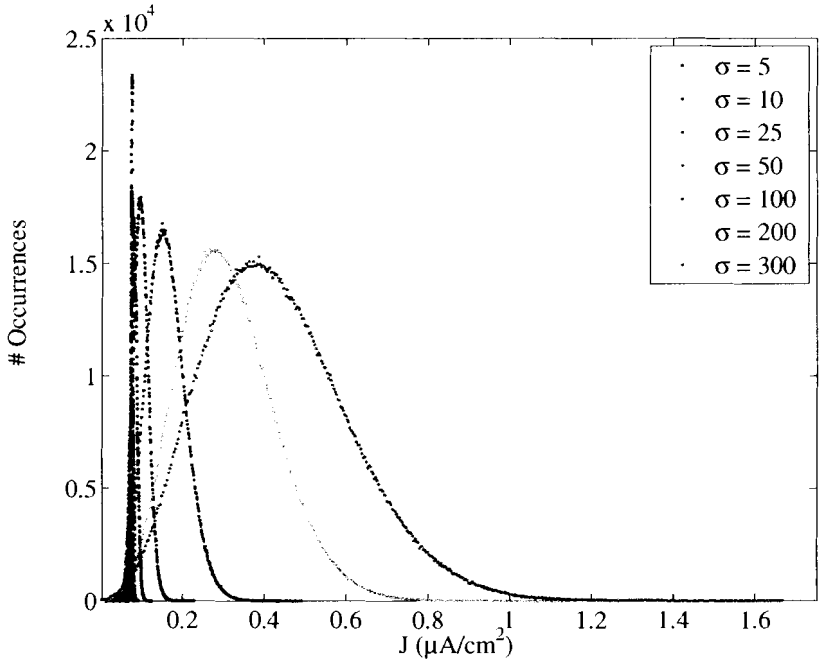

Figure 4.16: Histogram showing how leakage current density shifts with σ for a 0.003 μm^2 capacitor using model B.

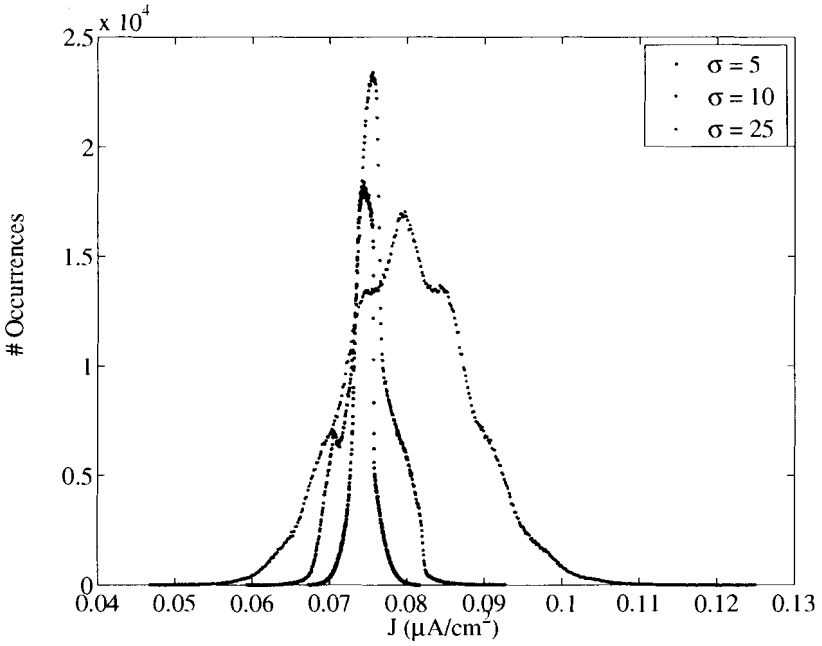

Figure 4.17: Histograms of the smallest standard deviation films from Figure 4.16

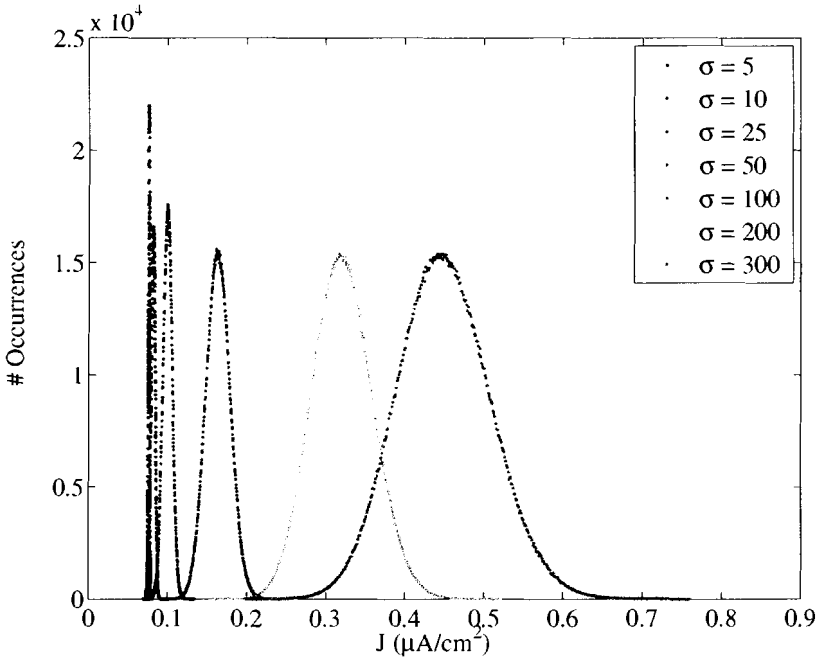

Figure 4.18: Histogram showing how leakage current density shifts with σ for a 0.03 μm^2 capacitor using the large variation model B.

Figure 4.19 shows only histograms for the films with standard deviations of 5 and 10 nm^2 from Figure 4.18. Both histograms show a wavy distribution. Possible reasons for this include the effects of adding outlier crystals to the capacitor, not having enough granularity in leakage model A for these tight distributions, or scaling.

Figure 4.20 shows how leakage current density is varying versus standard deviation for the 0.3 μm^2 capacitor. The range of variation in these films for each standard deviation is low, and the mode values appear unchanged from Figure 4.18. The magnitude of leakage current density and variation is much greater than that found in leakage model A for the same size capacitor. The histograms appear Gaussian instead of lognormal. Another interesting trait is how distinct each histogram is - there's a large separation between films from the σ = 50 nm^2 film and up.

Figure 4.21 shows only histograms for the films with standard deviations of 5 and 10 nm^2 from Figure 4.20. The histogram for a standard deviation of 10 nm^2 appears

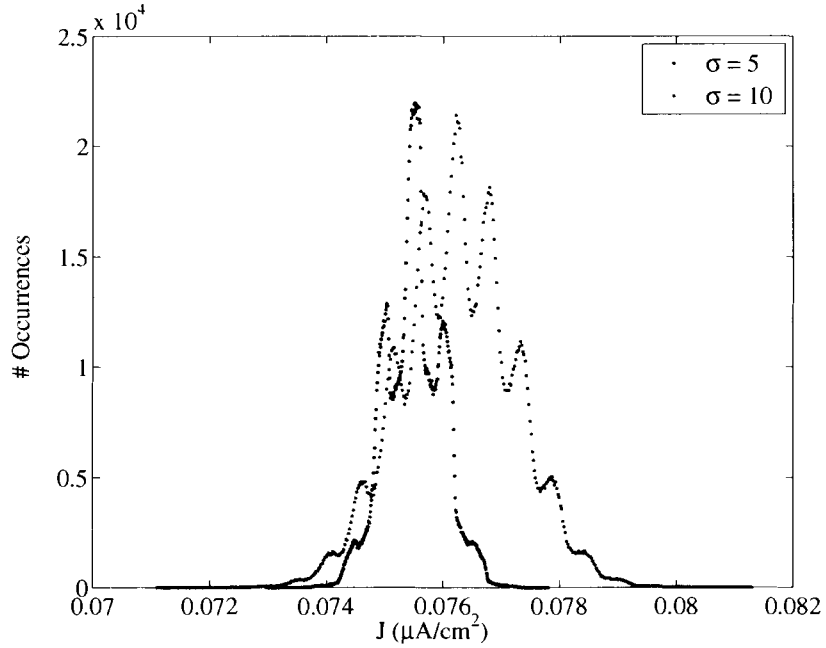

Figure 4.19: Histograms showing σ = 5 and σ = 10 from Figure 4.18

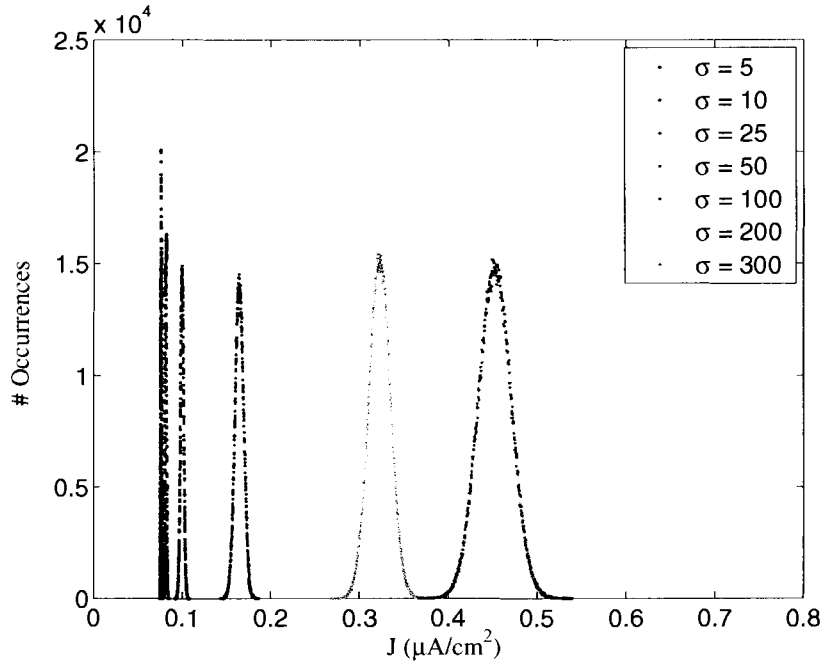

Figure 4.20: Histogram showing how leakage current density shifts with σ for a 0.3 μm^2 capacitor using the large variation model B.

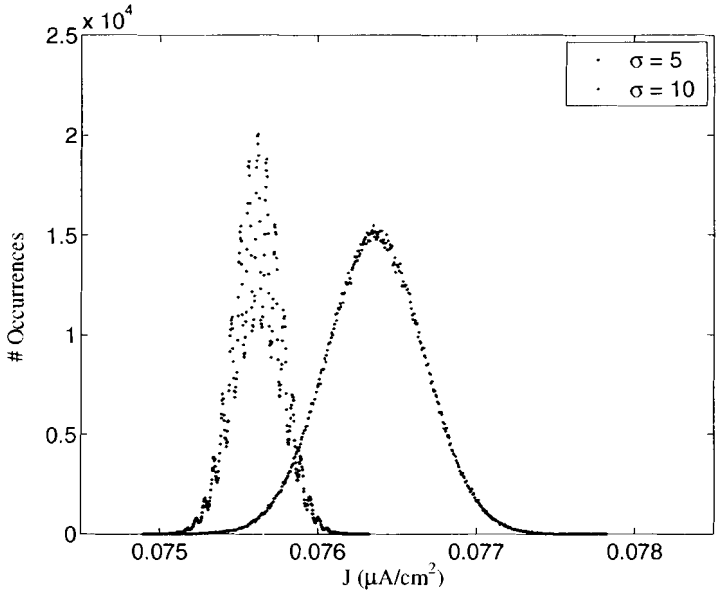

Figure 4.21: Histograms showing σ = 5 and σ = 10 from Figure 4.20

normal, but the histogram for a film with a standard deviation of 5 has an indistinct line. It appears similar to the dual distributions in Figure 4.14, with the upper boundary corresponding to the top line and the lower boundary to the bottom line. It is suspected that this is also due to oversampling of the data.

Percent variation of leakage current density is shown versus σ for the three capacitor areas in Figure 4.22. The leakage density in this model varies more than that of any other parameter, and it increases more than any other parameter when capacitor area is decreased. This graph doesn't show any lognormal tendencies. Leakage model A varies less than leakage model B - possibly leakage model A is linear enough for most standard deviations to produce lognormal outputs, while leakage model B is too nonlinear.

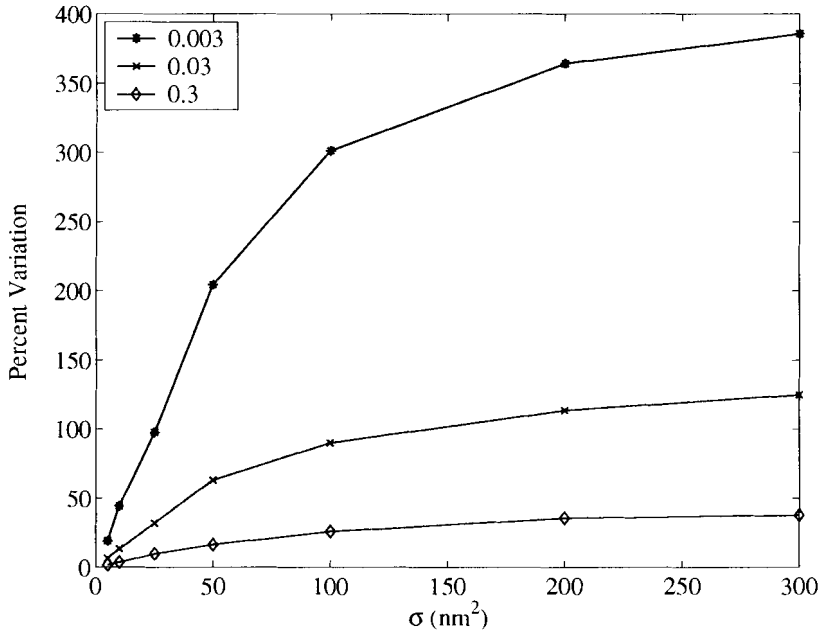

Figure 4.22: Percentage variation of leakage values for three different capacitor areas using the widely varying leakage model B.

CHAPTER 5

CONCLUSIONS AND FUTURE WORK

5.1 Conclusions

This thesis has detailed a method for evaluating the variability of a polycrystalline columnar thin film capacitor. A probability density function determined from experimental crystal area data was used, as well as a more easily manipulated lognormal probability density function. Equations have been derived relating a crystal's capacitance and leakage to its physical dimensions. Two leakage models were defined. Model A represented a best case where leakage was more linear. Model B represented a more exponential relationship between area and leakage. The Monte Carlo simulation code which took this data and simulated entire capacitors using these equations was outlined. Finally, results of the simulations have been analyzed to see how generated capacitors vary as the capacitor area and standard deviation of crystal area are varied.

The results obtained using the experimental distribution were that capacitance variation decreased from 47% to 3% as the average number of crystals per capacitor increased from 10 to 1000. The smaller variation leakage model A produced capacitors whose leakage varied from 0.1% to ~30% as the capacitor area decreased from 0.1 to 0.001 μm^2, while the larger variation leakage model B produced capacitors whose leakage varied from 59% to 644% over the same range. The lognormal distributions produced variations in capacitance ranging from 0.27% for a 0.3 μm^2 capacitor with a standard deviation of 5 nm^2 to 129% for a 0.003 μm^2 capacitor with a standard deviation of 300 nm^2. Leakage variations were even more diverse. Leakage model A produced variations ranging from 0.09% for a 0.3 μm^2 capacitor with a standard deviation of 5 nm^2 to 12.1% for a 0.003 μm^2 capacitor with a standard deviation of 100 nm^2. Leakage model B produced variations ranging from 1.9% for a 0.3 μm^2 capacitor with a standard

deviation of 5 nm^2 to 386% for a 0.003 μm^2 capacitor with a standard deviation of 300 nm^2. Tables 5.1, 5.2, and 5.3 show complete percent variation data for capacitance and leakage models A and B respectively found using the lognormal crystal area distribution.

It's difficult to compare the results to experimental data since researchers have concentrated on characterizing how BST electrical properties vary with regard to other process or environmental properties, ignoring intrinsic variation. By studying BST films prepared with a variety of deposition techniques and electrodes, others have found average dielectric constants that ranged from 140 to 600. Leakage current densities varied from 10^{-9} to $2*10^{-6}$ A/cm^2, with the majority being found in the low 10^{-8} [1]. Still, by estimating averages and calculating variation, these show a 124% variation in dielectric constants and a remarkable 9995% variation in leakage, so the numbers generated by this study are reasonable.

This work attempted to provide insight into how a capacitor with a polycrystalline dielectric will vary independent of process variations. Unlike amorphous dielectrics, capacitors with polycrystalline dielectrics will have innate variations in capacitance and leakage due to the area dependence of these parameters in individual crystals. The results show that if either electrical properties or crystal area probability are nicely behaved (i.e.; they do not get large or small quickly at extremes) then the final products will be well behaved. Using data from the lognormal distribution with a mean and standard deviation of 100 nm^2, it should be possible to generate capacitors as small as 500 nm^2 whose capacitance varies less than 18.9% and whose leakage varies between less than 2.1% and less than 71.3%. Rather than trying to eliminate crystal area variation, process engineers should concentrate on making sure such variation is well – behaved.

Capacitor Area (nm^2)	σ (nm^2)						
	5	10	25	50	100	200	300
10	4.94	9.80	25.97	56.16	102.44	131.80	143.24
15	3.89	7.59	21.10	48.46	90.01	124.75	136.82
20	3.45	7.27	19.73	40.83	83.90	124.02	134.40
25	3.03	6.12	16.77	35.74	79.46	120.87	132.42
30	2.86	5.91	14.74	33.81	74.35	113.45	128.66
35	2.49	5.19	14.74	30.54	67.39	108.93	122.46
40	2.41	4.93	12.73	28.54	68.87	101.13	122.59
50	2.23	4.61	11.79	24.74	61.09	92.03	114.87
60	1.96	4.26	10.31	24.09	55.48	88.44	106.35
70	1.86	3.87	10.21	21.51	51.71	83.93	102.59
80	1.75	3.55	10.38	19.84	46.09	79.56	98.47
90	1.62	3.29	8.59	19.42	44.36	77.75	95.06
100	1.53	3.22	8.59	18.23	45.67	74.85	88.14
150	1.28	2.67	6.79	14.76	34.86	63.35	73.65
200	1.10	2.26	5.72	12.74	30.78	53.75	69.13
300	0.91	1.87	4.74	11.06	24.36	43.56	56.08
400	0.77	1.49	4.02	9.15	22.05	39.73	50.03
500	0.70	1.37	3.72	8.30	18.89	34.17	44.52
600	0.60	1.28	3.46	7.47	18.53	32.97	41.71
700	0.56	1.17	3.23	6.77	17.21	31.91	39.44
800	0.55	1.15	2.80	6.65	16.18	27.60	35.86
900	0.50	1.03	2.63	5.94	14.05	24.63	33.76
1000	0.46	0.98	2.56	5.79	12.67	24.93	29.61
2000	0.32	0.73	1.75	4.22	9.92	18.36	22.74
3000	0.26	0.54	1.46	3.01	8.00	14.49	17.78

Table 5.1: Percent variation for capacitance.

Capacitor Area (nm^2)	σ (nm^2)						
	5	10	25	50	100	200	300
10	9.52	11.98	17.49	23.62	22.98	15.26	11.87
15	6.96	8.56	13.30	18.01	18.69	12.73	10.40
20	5.35	6.72	10.44	14.87	15.59	11.29	9.11
25	4.39	5.49	8.60	13.32	13.67	10.39	8.36
30	3.62	4.66	7.48	11.15	12.07	9.42	7.70
35	3.13	4.02	6.80	9.86	11.46	8.57	7.11
40	2.84	3.67	6.23	9.05	10.62	7.75	6.50
50	2.31	3.01	5.21	7.76	9.18	6.86	5.81
60	1.94	2.68	4.52	7.00	7.92	6.37	5.40
70	1.71	2.33	4.16	5.96	6.99	5.75	4.96
80	1.54	2.01	3.55	5.29	6.77	5.26	4.49
90	1.36	1.86	3.38	5.14	5.99	5.05	4.20
100	1.24	1.69	2.98	4.72	5.69	4.67	3.90
150	0.87	1.22	2.46	3.49	4.42	3.67	3.07
200	0.72	0.97	1.87	2.99	3.50	2.95	2.73
300	0.49	0.79	1.38	2.36	2.82	2.35	2.11
400	0.39	0.58	1.20	2.04	2.34	2.03	1.78
500	0.33	0.50	1.00	1.65	2.07	1.83	1.57
600	0.30	0.45	0.99	1.47	1.96	1.63	1.36
700	0.26	0.40	0.89	1.35	1.80	1.46	1.27
800	0.23	0.39	0.72	1.26	1.74	1.33	1.21
900	0.21	0.34	0.69	1.17	1.40	1.22	1.04
1000	0.19	0.32	0.66	1.11	1.29	1.18	0.97
2000	0.12	0.21	0.43	0.80	0.91	0.81	0.72
3000	0.09	0.16	0.36	0.55	0.74	0.63	0.57

Table 5.2: Percent variation for leakage model A.

Capacitor Area (nm^2)	σ (nm^2)						
	5	10	25	50	100	200	300
10	41.90	68.66	162.90	343.01	486.34	622.48	618.49
15	34.55	58.36	135.29	252.02	387.38	498.64	516.85
20	27.62	53.49	119.22	227.30	370.29	426.03	471.15
25	22.60	44.30	106.10	205.57	303.09	404.50	393.55
30	19.26	44.49	97.63	204.53	301.16	364.29	385.63
35	17.15	37.02	97.67	176.04	275.20	342.61	358.05
40	17.65	36.24	84.59	148.69	243.08	342.93	331.08
50	16.80	34.99	77.97	133.29	223.01	296.14	295.19
60	15.06	31.41	72.15	134.18	197.51	258.02	273.04
70	13.75	26.87	65.19	116.21	186.65	255.75	262.70
80	12.14	27.46	59.90	115.61	169.78	228.40	239.99
90	11.37	23.04	61.15	108.38	164.63	225.04	229.24
100	10.78	23.18	58.39	101.02	158.95	208.70	218.70
150	9.29	17.55	44.43	79.09	128.78	161.16	184.08
200	7.77	16.00	36.97	67.52	115.27	141.16	158.50
300	6.40	13.39	31.94	63.16	90.02	113.53	124.78
400	5.50	10.69	26.97	48.28	85.22	104.92	107.11
500	5.09	9.68	23.87	46.89	71.32	87.52	101.47
600	4.45	8.94	22.51	39.40	66.47	89.92	86.36
700	3.95	8.05	20.26	36.88	61.01	75.07	82.85
800	3.93	8.23	18.96	33.15	55.04	67.20	74.79
900	3.54	7.24	17.17	32.16	53.96	66.84	73.32
1000	3.25	6.71	16.03	29.91	49.08	61.25	68.30
2000	2.34	4.93	11.20	22.36	37.26	43.98	45.12
3000	1.89	3.76	9.95	16.58	25.94	35.66	37.85

Table 5.3: Percent variation for leakage model B.

5.2 Future Work

There is a great deal of work remaining on this project. Acquiring more data on crystal area variation and the area's relationship to capacitance and leakage would be useful. This data could be used to refine the equations in Chapter 2 and include realistic process variations in the models. The Monte Carlo simulation could incorporate a way of including fractions of crystals under the electrodes, thus eliminating the reduction of results if the area goes over. Crystal geometry could be considered; leakage current can flow along the outside of the grain, so a crystal with a wrinkled, irregular shape should produce more leakage current than one with identical area but smooth, cylindrical size. This simulation could be made more relevant to the DRAM industry by incorporating a simulated transistor with a polycrystalline gate attached as shown in Figure 1.2. Finally, devices could be manufactured, tested, and the results compared to see how accurate these simulations are.

REFERENCES

[1] S. Ezhilvalavan and T. Tseng, "Progress in the development of (Ba,Sr)TiO_3 (BST) thin films for Gigabit era DRAMs," *Materials Chemistry and Physics*, vol. 65, no. 3, pp. 227–248, 2000.

[2] D. E. Kotecki, J. D. Baniecki, H. Shen, R. B. Laibowitz, K. L. Saenger, J. J. Lian, T. M. Shaw, S. D. Athavale, C. Cabral, Jr., P. R. Duncombe, M. Gutsche, G. Kunkel, Y. Park, and R. Wise, "$Ba_{0.7}Sr_{0.3}TiO_3$ dielectrics for future stacked-capacitor DRAM," *IBM Journal of Research and Development*, vol. 43, pp. 367–382, May 1999.

[3] G. W. Dietz, M. Schumacher, R. Waser, S. K. Streiffer, C. Basceri, and A. Kingon, "Leakage currents in $Ba_{0.7}Sr_{0.3}TiO_3$ thin films for ultrahigh-density dynamic random access memories," *Journal of Applied Physics*, vol. 82, pp. 2359–2364, Sept. 1997.

[4] T. Hamamoto, S. Sugiura, and S. Sawada, "On the retention time distribution of dynamic random access memory (dram)," *Journal of Applied Physics*, vol. 45, pp. 1300–1309, Sept. 1996.

[5] A. Hiraiwa, M. Ogasawara, N. Natsuaki, Y. Itoh, and H. Iwai, "Statistical modeling of dynamic random access memory data retention characteristics," *IEEE Trans. Electron Devices*, vol. 80, pp. 3091–3099, June 1998.

[6] P. Restle, J. W. Park, and B. F. Lloyd, "DRAM variable retention time," in *IEDM Proc.*, pp. 807–810, Apr. 1992.

[7] A. Y. Romanenko and W. M. Gosney, "A numerical analysis of the storage times of dynamic random-access memory cells incorporating ultrathin dielectrics," *IEEE Trans. Electron Devices*, vol. 45, pp. 218–223, Jan. 1998.

[8] M. Ogasawara, Y. Ito, M. Muranaka, Y. Yanagisawa, Y. Tadaki, N. Natsuaki, T. Nagata, and Y. Miyai, "Physical model of bit-to-bit variation in data retention time of DRAMs," in *53rd Annual Device Research Conference Digest*, (Charlottesville, Virginia), pp. 164–165, June 1995.

[9] N. Shigyo, N. Wakita, T. Morishita, K. Sugawara, and Y. Asahi, "Technology cad based statistical simulation of mostfets," *Solid-State Electronics*, vol. 44, pp. 1001–1007, 2000.

[10] J. Cousins and D. Kotecki, "Simulation of the variability in microelectronic capacitors having polycrystalline dielectrics," *IEEE Electron Device Letters*, vol. 23, pp. 267–269, May 2002.

[11] J. Cousins and D. Kotecki, "Simulation of the variability in next–generation microelectronic capacitors with polycrystalline dielectrics," in *MRS Ferroelectric Thin Films X*, vol. 688, (Boston), pp. 247–252, Nov. 2001.

APPENDIX

Matlab and C Code

This appendix includes all the code used to prepare statistical distributions and perform Monte Carlo simulations.

Matlab Scripts

Data Generation Script

This script generates ϵ_r, capacitance, and leakage data for statistical data stored in array $rand1$

```
esubr1=(200/46)*(sqrt(4*rand1/pi))+30;%numbers from Dietz
                                      %leakage I in BST.
J1a=4.83*10^-14.*exp(126.8./sqrt(esubr1));% leakage
                                          % in A/cm^2
J1b=3.33*10^-08*exp(5.74./sqrt(esubr1));
```

Lognormal Data Generation Script

Similar to Section 5.2, this script also generates crystal areas with a lognormal distribution. The distribution is made by passing a mean and standard deviation to the program. To get values for the data files, each y-value in the probability density function is scaled up by const to produce values larger than one. The scaling factor is found by guessing values that would generate a total array size between 223,000 and 273,000.

```
%inputs: xstd, xmean-desired std and mean, option =
%functionality of script
%This code takes a mean and standard deviation, along with
%a code number to determine the functionality of the script.
```

```
%It can generate all the source data needed for a
%simulation run using a lognormal crystal area distribution.


xmeangen=0; %initiallize variables
xstdgen=0;
S=sqrt(log((xstd^2)/(xmean^2)+1));  %Set lognorm parameters
M=log(xmean)-(S^2)/2;
xxx=linspace(.1,(xmean+10*xstd),10000);
Fx=(1/2).*(1+erf((log(xxx)-M)./(S.*sqrt(2)))); %cdf
fx=(1./(S.*xxx.*(sqrt(2*pi)))).*exp(-(log(xxx)-M).^2
fx=fx./(2.*S^2));                          %pdf
Fx=Fx./Fx(end);                            %normallization
fx=fx./(((xxx(2)-xxx(1)))*trapz(fx));
fx=round(fx.*const);%scale up to generate arrays of
                    %certain size
k=1;
if (option >= 1)  %option <1 is just generating lognorm
xx=0;
fxx=0;
for l=1:1:length(fx)    %screen out 0's in array
if fx(l)~=0      %if value not equal to 0
fxx(k)=fx(l);
xx(k)=xxx(l);
k=k+1;
end
end

if (option >=2) %option >=2 also generates the array of
clear randx;    %lognormally distributed crystal areas and
randx=0;        %the electrical properties of each xtal
for n=1:1:length(xxx)
for m=1:1:fx(n)
randx(length(randx)+1)=xxx(n);
end
end
randx=sort(randx);
randx=randx(2:end);
esubrs=(200/46)*(sqrt(4*randx/pi))+30;
Jas=4.83*10^-14.*exp(126.8./sqrt(esubrs));  %A/cm^2
Jbs=3.33*10^-08*exp(5.74./sqrt(esubrs));
caps=(8.85*10^-3).*esubrs.*randx./10;  %C=er*eo*A/d
end
end
```

Lognormal Input Data Preparation Script

This script makes extensive use of the Lognormal Data Generation Script to prepare all the files needed to perform simulations that vary both distribution standard deviation and capacitor area.

```
%Requires no inputs
%Generates input data for simulation - all const values
%were empirically found so output arrays would have values
%between 223,000 and 273,000 entries.  This code was
%created to automate the data creation process - writing
%data takes an inconveniently long time.

xmean=100;  % initiallize variables
xmeangen=0;
xstdgen=0;


xstd=5      %std dev in nm^2
const=3500; %arbitrary constant
distsig     %routine to generate lognormal dist
dlmwrite('size5.dat',randx,'\n')    %write the data
dlmwrite('cap5.dat',caps,'\n')
dlmwrite('ja5.dat',Jas.*randx,'\n') %current density
                                    %times area
dlmwrite('jb5.dat',Jbs.*randx,'\n') %yields current.
%C code takes grain leakage current, adds all grains,
%divides by total area

xstd        %print out the std dev of the distribution
xstd=10     %you've just finished writing
const=4500;
distsig
dlmwrite('size10.dat',randx,'\n')
dlmwrite('cap10.dat',caps,'\n')
dlmwrite('ja10.dat',Jas.*randx,'\n')
dlmwrite('jb10.dat',Jbs.*randx,'\n')

%
xstd
xstd=25
const=8000;
```

```
distsig
dlmwrite('size25.dat',randx,'\n')
dlmwrite('cap25.dat',caps,'\n')
dlmwrite('ja25.dat',Jas.*randx,'\n')
dlmwrite('jb25.dat',Jbs.*randx,'\n')

%
xstd
xstd=50
const=14000;
distsig
dlmwrite('size50.dat',randx,'\n')
dlmwrite('cap50.dat',caps,'\n')
dlmwrite('ja50.dat',Jas.*randx,'\n')
dlmwrite('jb50.dat',Jbs.*randx,'\n')

%
xstd
xstd=100
const=30000;
distsig
dlmwrite('size100.dat',randx,'\n')
dlmwrite('cap100.dat',caps,'\n')
dlmwrite('ja100.dat',Jas.*randx,'\n')
dlmwrite('jb100.dat',Jbs.*randx,'\n')

%
xstd=200;
const=50000;
distsig
dlmwrite('size200.dat',randx,'\n')
dlmwrite('cap200.dat',caps,'\n')
dlmwrite('ja200.dat',Jas.*randx,'\n')
dlmwrite('jb200.dat',Jbs.*randx,'\n')

%
xstd
xstd=300;
const=70000;
distsig
dlmwrite('size300.dat',randx,'\n')
dlmwrite('cap300.dat',caps,'\n')
dlmwrite('ja300.dat',Jas.*randx,'\n')
dlmwrite('jb300.dat',Jbs.*randx,'\n')
```

```
%The distributions for std dev = 500 and 1000 were
%examined but produced such unrealistic probability
%density functions that they were discarded.

%
%xstd
%xstd=500;
%const=115000;
%distsig
%dlmwrite('size500.dat',randx,'\n')
%dlmwrite('cap500.dat',caps,'\n')
%dlmwrite('ja500.dat',Jas.*randx,'\n')
%dlmwrite('jb500.dat',Jbs.*randx,'\n')
%
%xstd=1000;
%distsig
%dlmwrite('size1000.dat',randx,'\n')
%dlmwrite('cap1000.dat',caps,'\n')
%dlmwrite('ja1000.dat',Jas.*randx,'\n')
%dlmwrite('jb1000.dat',Jbs.*randx,'\n')
```

Data Retrieval Script

This script pulled and organized data from ASCII text files into Matlab. A few different versions of this code exist to take into account differences in the file structure of different runs – the simulation of the extracted distribution didn't require the "for" loop shown below, since there was only one probability density function and thus only one set of outputs.

```
%Pulls data

capnames=['capval_005.txt';'capval_010.txt';...
'capval_025.txt';'capval_050.txt';'capval_100.txt';...
'capval_200.txt';'capval_300.txt'];
janames=['ja_005.txt';'ja_010.txt';'ja_025.txt';...
'ja_050.txt';'ja_100.txt';'ja_200.txt';'ja_300.txt'];
jbnames=['jb_005.txt';'jb_010.txt';'jb_025.txt';...
'jb_050.txt';'jb_100.txt';'jb_200.txt';'jb_300.txt'];
numxtalnames=['numxtal_005.txt';'numxtal_010.txt';...
'numxtal_025.txt';'numxtal_050.txt';'numxtal_100.txt';...
```

```
'numxtal_200.txt';'numxtal_300.txt'];

n=1;
capminmax=reshape(1:10,1,10); %the reshape calls initialize
jaminmax=reshape(1:10,1,10);  %each value as a 3D matrix.
jbminmax=reshape(1:10,1,10);  %They have no other purpose.
numxtalminmax=reshape(1:10,1,10);
xcaphist=reshape(zeros(8,500),8,500);
ycaphist=reshape(zeros(8,500),8,500);
xjahist=reshape(zeros(8,500),8,500);
yjahist=reshape(zeros(8,500),8,500);
xjbhist=reshape(zeros(8,500),8,500);
yjbhist=reshape(zeros(8,500),8,500);
for m=1:1:7 % do for each probability density function
  capsval=dlmread(capnames(n,:),'\n');%pulling data
  jas=dlmread(janames(n,:),'\n');
  jbs=dlmread(jbnames(n,:),'\n');
  numxtals=dlmread(numxtalnames(n,:),'\n');
%  sizes=dlmread(sizenames(n,:),'\n')
%  Stopped tracking crystal size

  sortcapsval=sort(capsval); %sorting data
  sortjas=sort(jas);
  sortjbs=sort(jbs);
  sortnumxtals=sort(numxtals);
%  sortsizes=sort(sizes);

  capsavg(n)=mean(capsval); %averaging data
  jasavg(n)=mean(jas);
  jbsavg(n)=mean(jbs);
  numxtalsavg(n)=mean(numxtals);

%getting cumulative sums of data
%  sizeavg(n)=mean(sizes);
%  cumsumcap(:,n)=cumsum(capval); %getting cumulative
%  cumsumja(:,n)=cumsum(ja(:,n));   %sums of data
%  cumsumjb(:,n)=cumsum(jb(:,n));

  %getting percentage variation
  percaps(n)=(sortcapsval(end)-sortcapsval(1));
  percaps(n)=percaps(n)/capsavg(n);

  perjas(n)=(sortjas(end)-sortjas(1))/jasavg(n);

  perjbs(n)=(sortjbs(end)-sortjbs(1))/jbsavg(n);
```

```
  %xxxminmax tracks 10 outlier values
  %n,1:5 are 5 smallest
  %n,end-4:end are 5 largest

  capsminmax(n,1:5)=sortcapsval(1:5)';
  capsminmax(n,6:10)=sortcapsval(end-4:end)';

  jasminmax(n,1:5)=sortjas(1:5)';
  jasminmax(n,6:10)=sortjas(end-4:end)';

  jbsminmax(n,1:5)=sortjbs(1:5)';
  jbsminmax(n,6:10)=sortjbs(end-4:end)';

  numxtalsminmax(n,1:5)=sortnumxtals(1:5)';
  numxtalsminmax(n,6:10)=sortnumxtals(end-4:end)';

%Make histograms of electrical properties versus area.
%Each histogram consists of 500 bins over the range of
%found values.
  [ycaphist(n,:),xcaphist(n,:)]=hist(sortcapsval,500);
  [yjahist(n,:),xjahist(n,:)]=hist(sortjas,500);
  [yjbhist(n,:),xjbhist(n,:)]=hist(sortjbs,500);
  [ynmxhist(n,:),xnmxhist(n,:)]=hist(sortnumxtals,500);
  n=n+1
  %free up some memory
  clear capsval jas jbs numxtals sortcapvals sortjas;
  clear sortjbs sortnumxtals;
end

%once data is done being retrieved, save it to a file
save sigdata2;
```

Monte Carlo Simulation Code

This version of the Monte Carlo simulation code is typical. This simulates multiple capacitor sizes and uses multiple probability density functions. An earlier version of the code used only one probability density function, and was virtually identical. The only changes were in the paths for data files (''<working-dir>\file''

instead of ''<working-dir>\<sigma>\file'') and the removal of the outer loop which loops through distributions.

```
//Polycrystalline capacitor Monte Carlo simulation code
//Code copyright 2002 Jesse Cousins
//

#include <stdlib.h>
#include <iostream.h>
#include <time.h>
#include <math.h>
#include <fstream.h>
#include <string.h>

void main()
{
double TotalSize[] = { 1000, 1500, 2000, 2500, 3000,
3500, 4000, 5000, 6000, 7000,
8000, 9000, 10000, 15000, 20000,
30000, 40000, 50000, 60000, 70000,
80000, 90000, 100000, 200000, 300000 };
//Total cap size in nm^2
const char * sizestr[]= {"_0010","_0015","_0020","_0025",
"_0030","_0035","_0040","_0050","_0060","_0070",
"_0080","_0090","_0100","_0150","_0200",
"_0300","_0400","_0500","_0600","_0700",
"_0800","_0900","_1000","_2000","_3000"};
const int numcap=100000; // 1/loopnum of # capacitors
 //to generate
const int loopnum=20;  // multiple of numcap to compute
const int capnum=25;  //number of capacitor sizes to
 //simulate
double totcrnum=0;  // total number of crystals in
 // all capacitors
float totavgcs=0;    // average crystal size in all
 // capacitors
//float totcrbndsz = 0;  // total area of crystal
 //boundaries in all caps
unsigned int basenum=time(0); // grab the time as a
// value to randomize
double finalcapsz[numcap]; // array that holds final
   // capacitor sizes
double finalcapvl[numcap]; // array that holds final
```

```
   //capacitor values
double finalcapnm[numcap]; // array that holds # xtals
   // in cap
double finalleaka[numcap];
double finalleakb[numcap];

 double * xtalsize;
 double * xtalcap;
 double * LeakageA;
 double * LeakageB;
 int numElem;
 int tInt=0;
 int i=0;
 int j=0;
 double tDbl;
 char filedir[10];
 const char size[]="/size.dat";
 const char cap[]="/cap.dat";
 const char leak1[]="/ja.dat";
 const char leak2[]="/jb.dat";
 char tempstring[25];
 int randnum=0;


 cout << "Please enter the working directory:"<<endl;
 cin >> filedir;
 strcpy(tempstring,filedir);
 strcat(tempstring,size);

 ifstream fin;
 fin.open(tempstring, ios::in);
 if(fin.fail())
    {
    cout<<"'size.dat' not found. Exiting."<< endl;
    exit(-1);
    }
 numElem = 0;
 while(!fin.eof())
    {
    fin>>tDbl;
    numElem++;
    }
 numElem--;
 xtalsize = new double[numElem];
 fin.clear();
```

```
 fin.seekg(ios::beg);
 for(i=0;i<numElem;i++)
    {
    fin>>tDbl;
    xtalsize[i] = tDbl;
    }
 fin.close();

 strcpy(tempstring,filedir);
 strcat(tempstring,cap);

 ifstream fin2;
 fin2.open(tempstring, ios::in);
 if(fin2.fail())
    {
    cout<<"'cap.dat' not found. Exiting."<< endl;
    exit(-1);
    }
 xtalcap = new double[numElem];
 fin2.seekg(ios::beg);
 for(i=0;i<numElem;i++)
    {
    fin2>>tDbl;
xtalcap[i]=tDbl;
}
 fin2.close();


 strcpy(tempstring,filedir);
 strcat(tempstring,leak1);

 ifstream fin3;
 fin3.open(tempstring, ios::in);
 if(fin3.fail())
    {
    cout<<"'ja.dat' not found. Exiting."<< endl;
    exit(-1);
    }
 LeakageA = new double[numElem];
 fin3.seekg(ios::beg);
 for(int i=0;i<numElem;i++)
    {
   fin3>>tDbl;
LeakageA[i]=tDbl;
}
```

```
 fin3.close();

 strcpy(tempstring,filedir);
 strcat(tempstring,leak2);

 ifstream fin4;
 fin4.open(tempstring, ios::in);
 if(fin4.fail())
    {
    cout<<"'jb.dat' not found. Exiting."<< endl;
    exit(-1);
    }
 LeakageB = new double[numElem];
 fin4.seekg(ios::beg);
 for(int i=0;i<numElem;i++)
{
fin4>>tDbl;
LeakageB[i]=tDbl;
}
 fin4.close();

int count;
for(count=0;count<capnum;count++)
{
 char capvalstr[]="/capval";
 char leak1valstr[]="/ja";
 char leak2valstr[]="/jb";
 char numxtalvalstr[]="/numxtal";
 char capsizestr[]="/capsize";
 char txt[]=".txt";
//creating the name of the output file that holds
// capacitance value
 strcpy(tempstring,filedir); //copy the working
// directory to the temporary string
 strcat(tempstring,capvalstr); //put on "capval"
 strcat(tempstring,sizestr[count]); //append on "_xxx",
//where xxx is the size
 strcat(tempstring,txt); //put on ".txt"
 strcpy(capvalstr,tempstring); //store the string
//"working_dir/capval_xxxx.txt" into capvalstr-reset
//for each cap size

 strcpy(tempstring,filedir); //creating the name of the
// output file that holds leakage A
 strcat(tempstring,leak1valstr);
```

```
 strcat(tempstring,sizestr[count]);
 strcat(tempstring,txt);
 strcpy(leak1valstr,tempstring);

 strcpy(tempstring,filedir); //creating the name of the
// output file that holds leakage B
 strcat(tempstring,leak2valstr);
 strcat(tempstring,sizestr[count]);
 strcat(tempstring,txt);
 strcpy(leak2valstr,tempstring);

 strcpy(tempstring,filedir); //creating the name of the
// output file that holds the number of grains in a cap
 strcat(tempstring,numxtalvalstr);
 strcat(tempstring,sizestr[count]);
 strcat(tempstring,txt);
 strcpy(numxtalvalstr,tempstring);

// strcpy(tempstring,filedir);//creating the name of the
// output file that holds capacitor size
// strcat(tempstring,capsizestr);//inactive because size
// is scaled to be exactly size desired
// strcat(tempstring,sizestr[count]);
// strcat(tempstring,txt);
// strcpy(capsizestr,tempstring);

srand(basenum); // change the rand() function starting
       //number so it'll have different results every time

randnum=numElem/RAND_MAX; //get the number of times
//numElem can be divided into RAND_MAX,
if((numElem%RAND_MAX)) //plus 1 if there's a remainder
{
randnum++;
}

for(j=0;j<loopnum;j++) //loop to get loopnum*numcap caps
{
int c=0;
while(c < numcap)
{
double scaling = 0; //scaling factor to make A=.3um^2
double crystalnum = 0;  // number of crystals in current cap
double capsize = 0;     // total cap size (nm^2)
double capval = 0;      // total capacitance(aF=10^-18 F)
```

```
double leaka = 0;
double leakb = 0;

while(capsize < TotalSize[count])  // keep going until
// you've got enough area for a capacitor of size TotalSize
{
tInt=0;
do
{
tInt=(rand() * randnum) + (rand() % randnum);
}
while(tInt>numElem);
//This gets a random number limited at the upper part to
//numElem, no more, no less-rand() gives 0 to 32767, so need
//so need to make sure a rand between 0 and numElem
//is generated

capsize = capsize + xtalsize[tInt]; // the crystal's
//area is added to total cap size
leaka=leaka +(LeakageA[tInt]);
leakb=leakb + (LeakageB[tInt]);
capval = capval + xtalcap[tInt];
crystalnum++; //counting var, # crystals in cap
}

//take leakage current per cap, translate into leakage
//current density (A/nm^2) to create the scaling factor,
//and scale electrical properties by the fractional
//reduction in cap size

leaka=leaka/(capsize);
leakb=leakb/(capsize);
scaling=TotalSize[count]/capsize;
capval=capval*scaling;

leaka=leaka*scaling;
leakb=leakb*scaling;
capsize=capsize*scaling;
finalcapsz[c] = capsize;
finalcapvl[c] = capval;
finalcapnm[c] = crystalnum;
finalleaka[c] = leaka;
finalleakb[c] = leakb;
c++; // increment # of capacitors
}
```

```
ofstream fvlout;
ofstream fnmout;
ofstream flaout;
ofstream flbout;
//ofstream fszout;

//fszout.open(capsizestr, ios::out | ios::app);
// if(fszout.fail())
// {
//  cout << "Error creating capsize.txt.  Exiting." << endl;
//  exit(-1);
// }
fvlout.open(capvalstr, ios::out | ios::app);
 if(fvlout.fail())
 {
    cout << "Error creating capval.txt.  Exiting." << endl;
    exit(-1);
 }
fnmout.open(numxtalvalstr, ios::out | ios::app);
 if(fnmout.fail())
 {
    cout << "Error creating numxtal.txt.  Exiting." << endl;
    exit(-1);
 }
 flaout.open(leak1valstr, ios::out | ios::app);
 if(flaout.fail())
 {
    cout << "Error creating ja.txt.  Exiting." << endl;
    exit(-1);
 }
  flbout.open(leak2valstr, ios::out | ios::app);
 if(flbout.fail())
 {
    cout << "Error creating jb.txt.  Exiting." << endl;
    exit(-1);
 }
for (int i=0;i<numcap;i++)
{
// fszout << finalcapsz[i] << endl;
fvlout << finalcapvl[i] << endl;
fnmout << finalcapnm[i] << endl;
flaout << finalleaka[i] << endl;
flbout << finalleakb[i] << endl;
}
```

```
//fszout.close();
fvlout.close();
fnmout.close();
flaout.close();
flbout.close();

}
cout << tempstring << " created." << endl;  //status report
}
}
```

Biography of the Author

Jesse Cousins was born in Bangor, Maine on April 26, 1978. He graduated from Mount Desert Island Regional High School in 1996. He attended WPI briefly before transferring to the University of Maine. He graduated from the University of Maine with a Bachelor of Science degree in Electrical Engineering in 2000.

In May 2000 he was enrolled for graduate study in Electrical Engineering at the University of Maine and served as a research assistant. His current research interests include microelectronics process as well as analog and RF wafer sort techniques. He is a member of IEEE and his interests include physical fitness and music. He is a candidate for the Master of Science degree in Electrical Engineering from The University of Maine in December 2003.